University of Arkansas, Fayetteville

ScholarWorks@UARK

Graduate Theses and Dissertations

12-2021

Grid Homology Invariants for Singular Legendrian Links

Richard Michael Shumate
University of Arkansas, Fayetteville

Follow this and additional works at: https://scholarworks.uark.edu/etd

 Part of the Numerical Analysis and Computation Commons

Citation

Shumate, R. M. (2021). Grid Homology Invariants for Singular Legendrian Links. *Graduate Theses and Dissertations* Retrieved from https://scholarworks.uark.edu/etd/4282

This Dissertation is brought to you for free and open access by ScholarWorks@UARK. It has been accepted for inclusion in Graduate Theses and Dissertations by an authorized administrator of ScholarWorks@UARK. For more information, please contact uarepos@uark.edu.

Grid Homology Invariants for Singular Legendrian Links

A dissertation submitted in partial fulfillment
of the requirements for the degree of
Doctor of Philosophy in Mathematics

by

Richard Michael Shumate
Liberty University
Bachelor of Science in Mathematics, 2015
University of Arkansas
Master of Science in Mathematics, 2017

December 2021
University of Arkansas

This dissertation is approved for recommendation to the Graduate Council.

Jeremy Van Horn-Morris, Ph.D.
Dissertation Director

Yo'av Rieck, Ph.D.
Committee Member

Matthew Clay, Ph.D.
Committee Member

Matthew Day, Ph.D.
Committee Member

Abstract

If Λ_1^* and Λ_2^* are two oriented singular Legendrian links that are Legendrian isotopic, we first construct isomorphic front diagram representations of Λ_1^* and Λ_2^* that have a natural allowable singular grid diagram associated to them. These allowable singular grid diagrams will always correspond to singular Legendrian links. The grid Legendrian invariants, $\lambda^{\pm}$, in the nonsingular grid homology theory have a natural extension to the singular grid theory, and are natural under the newly defined singular grid moves. This gives an invariant of singular Legendrian links, and in fact, a broader class of singular links.

Acknowledgements

There are many wonderful people who have helped me through this journey.

First, I want to give thanks to my dissertation committee for their helpful feedback, and to my advisor Jeremy Van-Horn Morris, in particular. Without his patience, guidance, and support none of this would have been possible.

I also want to thank Max Planck Institute for Mathematics for their financial support and inviting me to spend time at their wonderful facility while my advisor spent his sabbatical there.

To my family and friends, I want to thank you all for your endless support and love. This feat would have been impossible without all of your encouragement and advice along the way.

Table of Contents

List of Figures

1 Introduction

Heegaard Floer homology is defined using Heegaard diagrams and applying Lagrangian Floer homology in a specific way ([22], [21]). If set up appropriately, a Heegaard diagram can represent a link in a 3-manifold, and the associated Heegaard Floer homology gives rise to an invariant of the link, called link Floer homology ([20], [23], [25]).

In [27], Sarkar and Wang showed that, for a certain class of Heegaard diagrams, the Heegaard Floer homology can be computed in a combinatorial way, and that, for any link L, there is an associated Heegaard diagram for which the link Floer homology of L can be computed combinatorially. After developing this idea further, in [11], Manolescu, Ozsváth, and Sarkar constructed a specific class of Heegaard diagrams which make computing link Floer homology fully a combinatorial task, using grid diagrams. In [12], Manolescu, Ozsváth, Szabó, and Thurston developed this grid homology theory to be a stand-alone theory, independent of the holomorphic construction. Though isomorphic to the link Floer homology, we will refer to the homology invariant coming from grid diagrams as grid homology.

Grid homology has connections to other link invariants, and can be used to provide a combinatorial proof of many relationships in knot theory. In particular, grid homology is useful in determining the Alexander polynomial, Seifert genus, slice genus, the unknotting number, among other knot or link invariants ([16], [17]).

In addition to having connections to various topological link invariants, there is a natural association of grid diagrams to front diagrams of Legendrian links in $\mathbb{R}^3$ with the standard contact structure $\xi_0 = \ker(dz - ydx)$. There are two generators of the grid chain complex whose homology classes are invariants of the underlying Legendrian link. Moreover, these invariants can be used to compute the classical Legendrian invariants and can even distinguish certain Legendrian non-simple knots ([10], [15], [24]).

As the invariants coming from the grid diagrams prove to be both computable and

powerful in distinguishing links in various settings, it is natural to try to extend these ideas to different settings. Variations of grid diagrams for singular objects have been explored in [29], [3], [1], [2], [8], and [18]. In particular, the construction due to Harvey-O'Donnol in [8] gives a grid diagram theory for transverse spatial graphs. They define graph grid diagrams, give a collection of graph grid moves, and define and prove invariance for the graph grid homology. Using this construction as the foundation, we define a grid diagram theory for oriented singular Legendrian links, from which two invariants $\lambda^{\pm}$ can be defined in a way as to generalize the grid invariants for Legendrian links, as first defined by Ozsváth, Szabó, and Thurston in [24].

Our construction is similar to the construction in [8], in that we utilize their proof of invariance of the graph grid homology for transverse spatial graphs, as we use a subcollection of the moves they prove invariance for. Our construction differs from their work in that we focus on the singular Legendrian setting, and describe the singular version of the grid invariants for Legendrian links.

In Section 5.1, we prove the following theorem to obtain a singular grid diagram representative for any singular Legendrian link and describe grid moves to relate isotopic singular Legendrian links.

Theorem 5.2. *If $\mathcal{G}_1^*$ and $\mathcal{G}_2^*$ are two singular grid diagrams representing Legendrian isotopic oriented singular Legendrian links, then $\mathcal{G}_1^*$ and $\mathcal{G}_2^*$ are related by a sequence of Legendrian grid moves (C and S:XNW, S:XSE) and singular Legendrian grid moves (C1*, C2*, CS:X*NW, CS:X*SE, RS:X*NW, RS:X*SE) in the torus.*

Applying Theorem 5.2, we then need to show that any move in the list of singular grid moves utilized in the theorem induces an isomorphism of graph grid homology, SGH^-, and which maps $\lambda^{\pm}(\mathcal{G}_1^*)$ to $\lambda^{\pm}(\mathcal{G}_2^*)$. To this end, we prove the following after some preliminary work,

Theorem 5.5. *Let $\mathcal{G}_1^*$ and $\mathcal{G}_2^*$ be singular grid diagrams representing isotopic oriented*

singular Legendrian links. Then there is an isomorphism $\phi : SGH^-(\mathcal{G}_1^*) \to SGH^-(\mathcal{G}_2^*)$ *where* $\phi(\lambda^+(\mathcal{G}_1^*)) = \lambda^+(\mathcal{G}_2^*)$ *and* $\phi(\lambda^-(\mathcal{G}_1^*)) = \lambda^-(\mathcal{G}_2^*)$.

In particular, we construct maps for the following diagram,

$$\begin{array}{ccccc} \Lambda_1^* & \overset{\sim}{\dashrightarrow} & \widetilde{\Lambda}_1^* & \longrightarrow & \mathcal{G}_{\widetilde{\Lambda}_1^*} \\ \Big\downarrow{\scriptstyle \text{Leg RM Move}} & & \Big\downarrow{\scriptstyle \text{Leg RM Moves}} & & \Big\downarrow{\scriptstyle \text{Sing Grid Moves}} \\ \Lambda_2^* & \overset{\sim}{\dashrightarrow} & \widetilde{\Lambda}_2^* & \longrightarrow & \mathcal{G}_{\widetilde{\Lambda}_2^*} \end{array}$$

where $\sim$ changes Λ^* into a Legendrian isotopic singular link with an allowable singular grid diagram. Then we show that the associated singular grid moves are natural with respect to the singular grid invariant.

While $\lambda^\pm$ are invariants of singular Legendrian links, the allowed singular grid moves do not always correspond to singular Legendrian isotopy, as will be discussed in more detail in Section 5.3. Due to this, $\lambda^\pm$ is an invariant of some larger unknown class of singular links, which is somewhere in between singular oriented Legendrian links and transverse spatial oriented Legendrian graphs.

Some further work could be done to discover what this larger class of links is, and see how the singular Legendrian invariant behaves in this class. Moreover, it would be interesting to develop the (relative) bigrading for SGH^- in this setting, determine how this can be useful for $\lambda^\pm$, and see if $\lambda^\pm$ can distinguish Legendrian simple oriented singular Legendrian links.

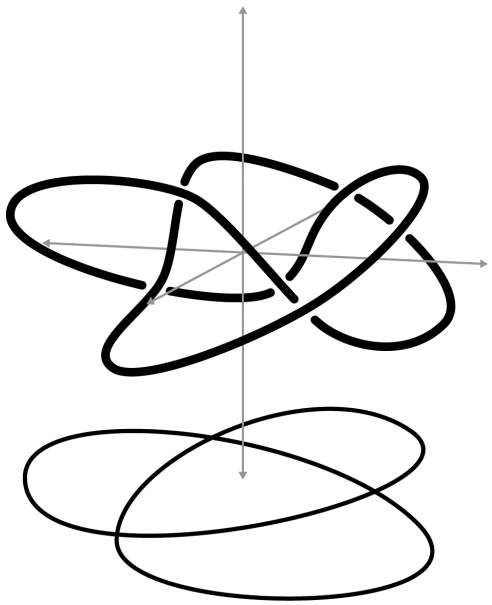

Figure 1: Generic Projection of a Knot Onto a Plane

2 Links and Grid Diagrams

For a given 3-manifold, M, an *oriented n-component link*, L, in M is a smooth embedding $\coprod^{n} S^1 \hookrightarrow M$, where an orientation on each copy of S^1 is specified. Links are considered up to *ambient isotopy*, that is, if L_1 and L_2 are two oriented links in M, an ambient isotopy from L_1 to L_2 is a function $H : M \times I \to M$ so that

1. $H_t(x) = H(x,t)$ is a diffeomorphism for each $t \in I$,
2. H_0 is the identity map on M,
3. $H_1(L_1) = L_2$ with correct orientation.

Ambient isotopy forms an equivalence relation on oriented links, and so the equivalence class of a link L under ambient isotopy is referred to as the *link class* of L. It is a classical question to determine all link classes in $\mathbb{R}^3$ (or S^3), and various 3-manifolds. To this end, a large number of invariants have been created that are useful in distinguishing link classes, which include grid homology, as we will discuss in detail.

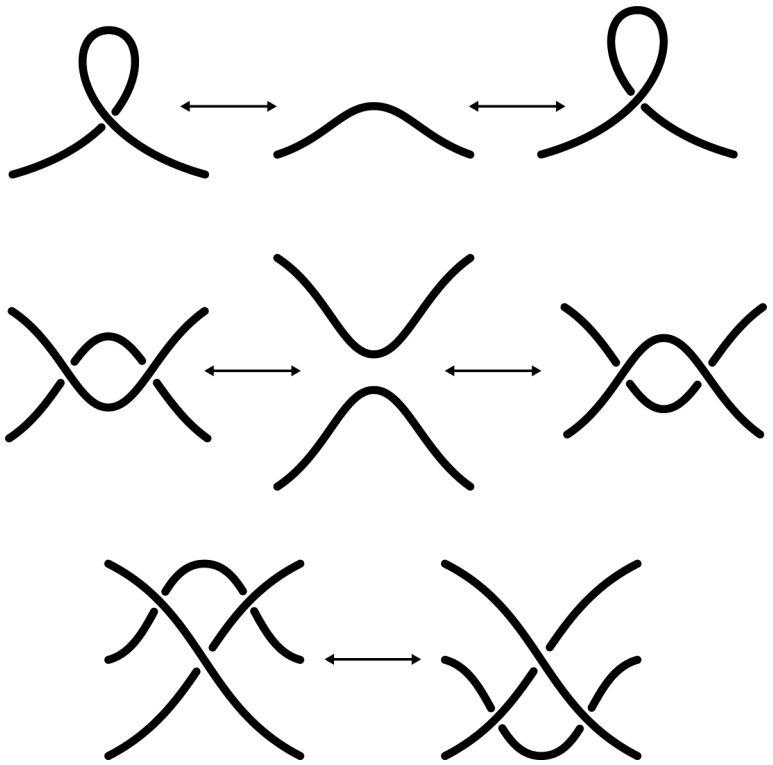

Figure 2: Three Different Reidemeister Moves

Two operations on links that will be particularly useful for the grid homology construction are that of mirroring and reversing. For an oriented link L, the *mirror* of L, denoted $m(L)$, is obtained by reflecting L through a plane in $\mathbb{R}^3$. The *reversal* of L, denoted $-L$ is obtained by switching the orientation on all components of L. In particular, mirrioring is used in the definition of grid homology for oriented Legendrian links and reversing orientation gives isomorphic grid homology invariants.

In order to simplify the study of links in $\mathbb{R}^3$, it is helpful to exchange ambient isotopies of links for a set of combinatorial moves on diagrams. To obtain a diagram representing an oriented link L, first take a generic orthogonal projection of L onto a plane in $\mathbb{R}^3$, which is an embedding except at finitely many transverse double points. To record the crossing information in the projection, a break is created in the strand involved in the formation of a double point which is the undercrossing strand in the 3-manifold. An arrow can be included on each component of the link in this diagram to keep track of the orientation of the link.

Pictured in Figure 2 are three generating moves of link diagrams, referred to as *Reidemeister moves*. For the purposes of labeling, we will refer to these moves and Reidemeister 1 ($RM1$), Reidemeister 2 ($RM2$), and Reidemeister 3 ($RM3$) moves, respectively. The complete list of Reidemeister moves for links includes any rotation of the three moves, and any crossing configuration of $RM3$. Though no orientation is specified in the figure, any consistent choice of orientation can be used with these moves. Notice that while considering the projection of a link L onto a plane, if a different plane is chosen, the diagram representing L can vary greatly. These local Reidemesiter moves resolve this well-definedness issue of diagrams according to the following fundamental theorem,

Theorem 2.1. *(Reidemeister, [26]) Two link diagrams represent ambient isotopic oriented links if and only if the diagrams are related by a finite sequence of planar isotopies and Reidemeister moves.*

When creating a link invariant, this theorem allows for invariance to be checked on the few local Reidemeister moves on diagrams instead of an ambient isotopy. In certain cases, this provides a drastic simplification of the proof of invariance.

2.1 Grid Diagrams and Grid Moves

A *grid diagram* $\mathcal{G}$ with grid size n is an $(n \times n)$ grid in $\mathbb{R}^2$ along with a set of X markings, $\mathbb{X}$, and a set of O markings, $\mathbb{O}$, so that

- each row contains exactly one X marking and each column contains exactly one X marking,
- each row contains exactly one O marking and each column contains exactly one O marking,
- any square in the grid contains at most one marking.

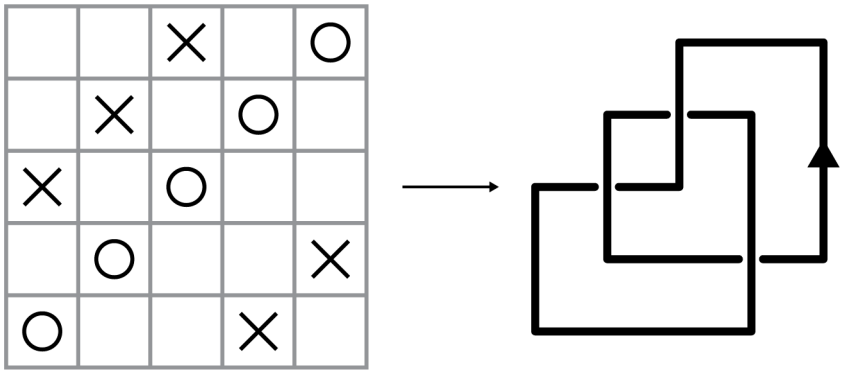

Figure 3: Grid Diagram representing 3_1

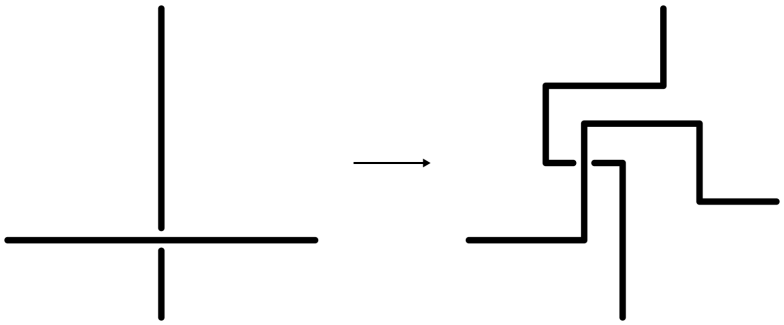

Figure 4: Local Modification for a Crossing in a Grid

Any grid diagram specifies a diagram for an oriented link. To construct the link diagram associated to a grid diagram, begin by drawing an oriented segment in each column from the X marking to the O marking. In each row, draw an oriented segment from the O marking to the X marking, creating breaks in the strand as necessary so that the horizontal segments are always the undercrossing segments. This specifies a piecewise-linear diagram, so if a smooth diagram is desired, smooth out the corner formed at each X and O marking. Moreover, every oriented link, L, has an associated grid diagram representing it. To construct such a grid diagram, approximate L with a piecewise-linear diagram admitting only vertical and horizontal segments. Any time a horizontal segment is an overcrossing, modify the diagram according to Figure 4. Move the link into a position where no segments are colinear, and then mark the turns with either an X or an O so that the vertical segments are oriented from the X marking to the O marking, and is consistent

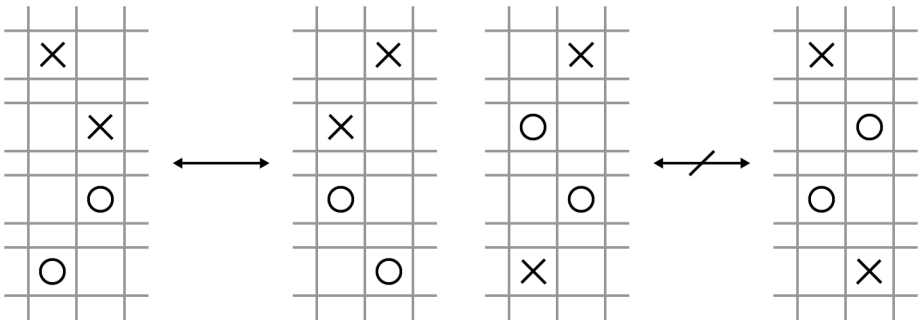

Figure 5: Valid and Invalid Column Commutations

with the orientation of L.

Just as there are Reidemeister moves to transition between diagrams of equivalent links, there is a set of moves that, when applied to a grid diagram, results in a new grid diagram where the underlying links are ambient isotopic.

Let C_i and C_{i+1} denote the ith and $(i+1)$st columns of a grid diagram $\mathcal{G}_1$. Let $I_j \subseteq \mathbb{R}$ denote the closed interval whose endpoints are the vertical positions of the X and O markings in C_j. A *column commutation* of $\mathcal{G}_1$ occurs by obtaining a new grid diagram $\mathcal{G}_2$ by swapping consecutive columns C_i and C_{i+1} of $\mathcal{G}_1$, provided one of the following conditions holds,

- $I_i \subset \text{Int}(I_{i+1})$,
- $I_{i+1} \subset \text{Int}(I_i)$,
- $I_i \cap I_{i+1} = \emptyset$.

In a similar way, one can define *row commutations* for consecutive rows R_i and R_{i+1} by considering intervals I_j whose endpoints are the horizontal position of the X and O markings in R_j. Either a column commutation or a row commutation will be referred to as a *commutation* and will be labeled as (C).

Let $\mathcal{G}_1$ be a grid diagram of size n. For a distinguished X marking in the (i,j)th square of $\mathcal{G}_1$, an *X-stabilization* of $\mathcal{G}_1$ is a grid diagram $\mathcal{G}_2$ of size $(n+1)$ obtained from $\mathcal{G}_1$ in the following way:

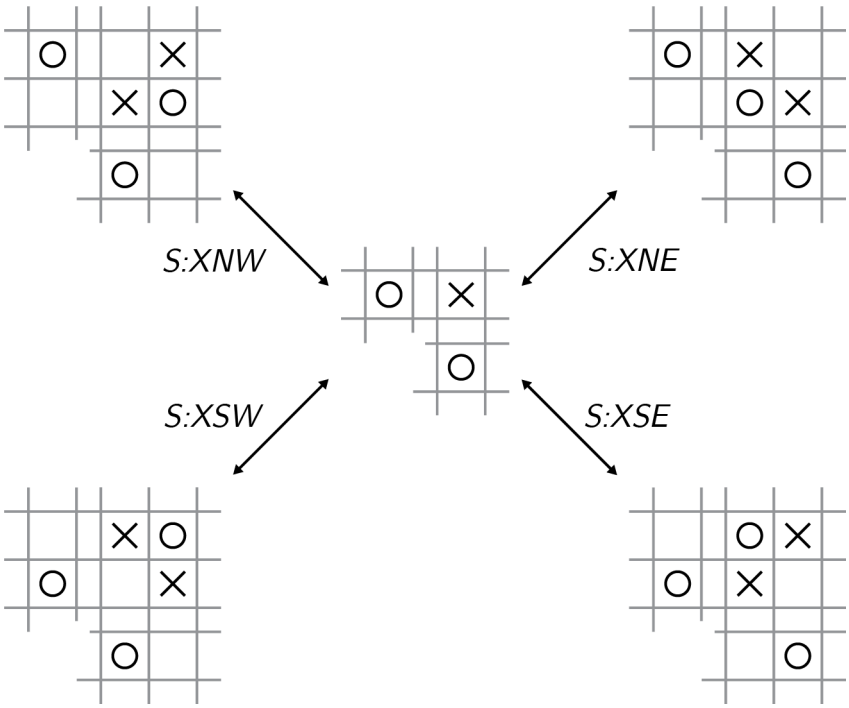

Figure 6: Stabilization options at an X marking

1. Remove the X marking in the (i, j)-th square, along with the O markings in the i-th row and in the j-th column.

2. Split the empty row and column into two rows and two columns by adding a vertical and horizontal line.

3. Replace the markings according to one of the four configurations pictured in Figure 6.

As seen in Figure 6, the different options for a stabilization at X are given a label according to the location of the empty square in the (2×2) box after stabilizing, as either $(S : XNW)$, $(S : XNE)$, $(S : XSW)$ or $(S : XSE)$. In an analogous way, one can define an *O-stabilization*, and will be labeled as either $(S : ONW)$, $(S : ONE)$, $(S : OSW)$, or $(S : OSE)$. Applying either an X- or an O-stabilization to a grid diagram $\mathcal{G}$ will be called a *stabilization* of $\mathcal{G}$, and applying the inverse of a stabilization to a grid diagram $\mathcal{G}$ will be called a *destabilization* of $\mathcal{G}$.

Collectively, column commutations, row commutations, stabilizations, and destabilizations

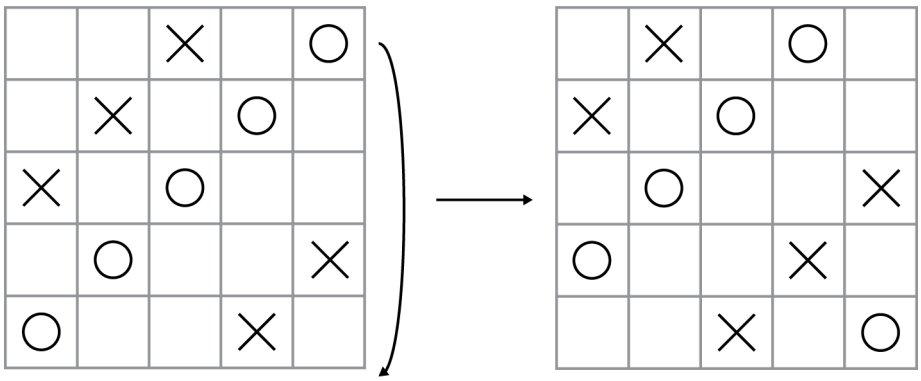

Figure 7: Cyclic Permutation from Top to Bottom

will be called *grid moves*, and the following theorem relates them to the standard Reidemesiter moves for links,

Theorem 2.2. *(Cromwell, [6]) Two planar grid diagrams represent equivalent links if and only if there is a finite sequence of grid moves that transforms one into the other.*

In addition to the standard grid moves, we will utilize one additional move, called cyclic permutation. Let $\mathcal{G}_1$ be a grid diagram of size n and let $\mathcal{G}_2$ be a new grid diagram obtained rearranging the columns of $\mathcal{G}_1$ in one of the following two ways,

- C_1 of $\mathcal{G}_2$ has the same configuration as C_n of $\mathcal{G}_1$ and C_j of $\mathcal{G}_2$ has the same configuration as C_{j-1} of $\mathcal{G}_1$, for $2 \leq j \leq n$.
- C_n of $\mathcal{G}_2$ has the same configuration as C_1 of $\mathcal{G}_1$ and C_j of $\mathcal{G}_2$ has the same configuration as C_{j+1} of $\mathcal{G}_1$, for $1 \leq j \leq n-1$.

In a similar way, one can define this move for rows, and when applied, $\mathcal{G}_2$ is said to be obtained from $\mathcal{G}_1$ by a *cyclic permutation*.

Proposition 2.3. *([24], Lemma 4.3) A cyclic permutation of planar grid diagrams can be realized by a sequence of commutation moves and stabilizations/destabilizations of types $(S:XNW)$, $(S:XSE)$, $(S:ONW)$, and $(S:OSE)$.*

Due to the above proposition, one can view a planar grid diagram as a diagram on the torus, where the top and bottom grid lines are identified and the left and right grid lines are identified. Doing so makes the horizontal and vertical grid lines horizontal and vertical circles. Viewing grid diagrams this way is beneficial, as the grid is now closely related to a Heegaard splitting.

The previous theorem also shows that cyclic permutations are redundant moves on the grid. That is, cyclic permutations can be realized by a sequence of other grid moves. In fact, there are more redundancies in the set of grid moves.

Proposition 2.4. *([24], Lemma 4.2) A stabilization of type $(S:ONE)$, $(S:ONW)$, $(S:OSE)$, and $(S:OSW)$, can be realized by a stabilization of type $(S:XSW)$, $(S:XSE)$, $(S:XNW)$, and $(S:XNE)$, respectively, with a sequence of commutations and cyclic permutations.*

Thus, based off of the theorems in this section, to prove invariance of the various homology theories, which will be defined in Sections 2.3 and 2.4, one needs to only prove invariance locally for commutations and stabilizations at X markings.

2.2 Grid States and Gradings

Let $\mathcal{G}$ be a grid diagram on the torus with grid size n. On the torus, the grid lines correspond to circles, and so, let $\boldsymbol{\alpha} = \{\alpha_i\}_{i=1}^n$ be the n horizontal circles and $\boldsymbol{\beta} = \{\beta_i\}_{i=1}^n$ be the n vertical circles which make up the grid for $\mathcal{G}$. A *grid state* for $\mathcal{G}$ is a n-tuple of points $\mathbf{x} = \{x_1, ..., x_n\}$ where the n points of $\mathbf{x}$ correspond to n of the n^2 intersections of $\boldsymbol{\alpha}$ and $\boldsymbol{\beta}$, so that each circle in $\boldsymbol{\alpha}$ and each circle in $\boldsymbol{\beta}$ contain exactly one of the points in $\mathbf{x}$. The set of all grid states for a grid diagram $\mathcal{G}$ will be denoted $\mathbf{S}(\mathcal{G})$.

The chain complexes, which define the various grid homology theories associated to $\mathcal{G}$, are generated by grid states. The differentials vary depending on the chosen theory, and will each be a count of certain rectangles between grid states.

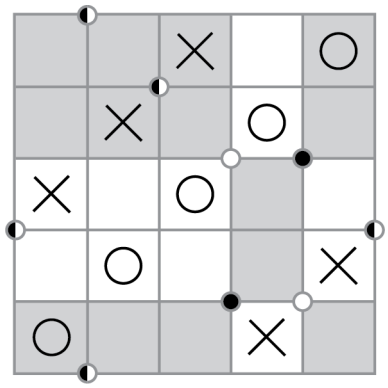

Figure 8: Grid Diagram with Two Grid States and Two Rectangles

For two grid states $\mathbf{x}, \mathbf{y} \in \mathbf{S}(\mathcal{G})$ a *rectangle* r from $\mathbf{x}$ to $\mathbf{y}$ is an embedded rectangle in the torus where

- $\partial r \subseteq \bigcup_{i=1}^{n} \alpha_i \cup \beta_i$,
- $\#(\mathbf{x} \cap \mathbf{y}) = n - 2$ and the corners of r are the four points not shared by $\mathbf{x}$ and $\mathbf{y}$,
- $\partial(\partial_{\boldsymbol{\alpha}} r) = \mathbf{y} - \mathbf{x}$ and $\partial(\partial_{\boldsymbol{\beta}} r) = \mathbf{x} - \mathbf{y}$, where $\partial_{\boldsymbol{\alpha}}$ and $\partial_{\boldsymbol{\beta}}$ denote the boundary of r intersected with the α and β curves, respectively.

The set of all rectangles from $\mathbf{x}$ to $\mathbf{y}$ will be denoted $\mathrm{Rect}(\mathbf{x}, \mathbf{y})$. Notice that either $\mathrm{Rect}(\mathbf{x}, \mathbf{y}) = \emptyset$ or $\#\mathrm{Rect}(\mathbf{x}, \mathbf{y}) = 2$. A rectangle $r \in \mathrm{Rect}(\mathbf{x}, \mathbf{y})$ is an *empty rectangle* if $\mathbf{x} \cap \mathrm{Int}(r) = \mathbf{y} \cap \mathrm{Int}(r) = \emptyset$. The set of empty rectangles from $\mathbf{x}$ to $\mathbf{y}$ will be denoted $\mathrm{Rect}^{\circ}(\mathbf{x}, \mathbf{y})$.

2.3 Fully Blocked Grid Homology for Knots

If $\mathcal{G}$ is a grid diagram, the *fully blocked grid chain complex* is the chain complex $(\widetilde{GC}(\mathcal{G}), \widetilde{\partial})$ where $\widetilde{GC}(\mathcal{G})$ is the $\mathbb{Z}_2$-vector space generated by $\mathbf{S}(\mathcal{G})$ and $\widetilde{\partial}$ is defined on generators by

$$\widetilde{\partial}(\mathbf{x}) = \sum_{\mathbf{y} \in \mathbf{S}(\mathcal{G})} \#\{r \in \mathrm{Rect}^{\circ}(\mathbf{x}, \mathbf{y}) \,|\, r \cap \mathbb{X} = r \cap \mathbb{O} = \emptyset\} \cdot \mathbf{y}.$$

In other words, $\widetilde{\partial}$ is the mod-2 count of empty rectangles which also do not contain any X or O markings. In this version of grid homology, the homology of the fully blocked chain complex is not an invariant of the link. Under stabilizations, the vector space changes dimensions. However, the following theorem extracts an invariant from this homology theory,

Theorem 2.5. *([12], Theorem 1.2, Proposition 2.14) If $\mathcal{G}$ is a grid diagram with grid size n that represents a knot, then the dimension $\dim_{\mathbb{Z}_2}\left(\widetilde{GH}(\mathcal{G})\right)/2^{n-1}$ is integer valued and an invariant of the underlying knot.*

This invariant stems from a deeper relationship between the fully blocked and simply blocked theories.

2.4 Unblocked Grid Homology and Simply Blocked Grid Homology for Knots

For a grid diagram $\mathcal{G}$ with grid size n, let $\mathcal{R} = \mathbb{Z}_2[V_1, ..., V_n]$ be the polynomial ring with variables $\{V_i\}_{i=1}^n$, which are in one-to-one correspondence with the O markings $\mathbb{O} = \{O_i\}_{i=1}^n$. Let $\mathcal{O}_i : \mathrm{Rect}(\mathbf{x}, \mathbf{y}) \to \{0, 1\}$ be defined as

$$\mathcal{O}_i(r) = \begin{cases} 0 & \text{if } O_i \notin r \\ \\ 1 & \text{if } O_i \in r \end{cases}.$$

For a grid diagram $\mathcal{G}$,the *unblocked grid chain complex* is the chain complex $(GC^-(\mathcal{G}), \partial^-)$ where $GC^-(\mathcal{G})$ is the $\mathcal{R}$-module generated by $\mathbf{S}(\mathcal{G})$, and ∂^- is defined on generators by

$$\partial^-(\mathbf{x}) = \sum_{\mathbf{y}\in\mathbf{S}(\mathcal{G})} \sum_{\{r\in \mathrm{Rect}^\circ(\mathbf{x},\mathbf{y}) \,|\, r\cap\mathbb{X}=\emptyset\}} V_1^{\mathcal{O}_1(r)} \cdots V_n^{\mathcal{O}_n}(r) \cdot \mathbf{y},$$

In this version notice that the empty rectangles are allowed to contain O markings, but anytime they intersect an O marking, the appropriate variable is included. Moreover,

notice that the following relationship holds,

$$\frac{GC^-(\mathcal{G})}{V_1 = \cdots = V_n = 0} = \widetilde{GC}(\mathcal{G}).$$

Lemma 2.6. *([12], Lemma 2.11) If $\mathcal{G}$ represents a knot, for any pair of integers $i, j \in \{1, ..., n\}$ multiplication by V_i is chain homotopic to multiplication by V_j.*

For a fixed $i \in \{1, ..., n\}$, the *unblocked grid homology* of $\mathcal{G}$ is the homology of $(GC^-(\mathcal{G}), \partial^-)$, as a module over $\mathbb{Z}_2[U]$ where the action of U is induced by multiplication by V_i.

The *simply blocked grid chain complex* is the quotient complex $\widehat{GC}(\mathcal{G}) = GC^-(\mathcal{G})/V_i$ for any $i \in \{1, ..., n\}$ and the simply blocked grid homology of $\mathcal{G}$ is the $\mathbb{Z}_2$-vector space obtained as the homology of $(\widehat{GC}(\mathcal{G}), \partial^-)$. Notice that the definition of $\widehat{GC}(\mathcal{G})$ is independent of choice of i, as multiplication by V_i is chain homotopic to multiplication by V_j, as stated in Lemma 2.6.

2.5 Invariance of Grid Homology for Knots

To see that these various grid homology theories result in invaraints of the underlying knots, we must show that, after applying either a commutation or an X-stabilization, the grid homology of the resulting grid diagram is the same. This section will lay out the road map for proof of invariance, but most of the detail will be deferred to [19].

Let $\mathcal{G}_1$ and $\mathcal{G}_2$ be two grid diagrams which are related by a column commutation that swaps columns C_i and C_{i+1}. To set up a homotopy equivalence between the grid homology of $\mathcal{G}_1$ and the grid homology of $\mathcal{G}_2$, we first view the two grid diagrams at the same time on a modified grid. Let $\boldsymbol{\alpha} = \{\alpha_1, ..., \alpha_n\}$ be the horizontal circles for $\mathcal{G}_1$ and $\boldsymbol{\beta} = \{\beta_1, ..., \beta_n\}$ be the vertical circles for $\mathcal{G}_1$. Since the commutation occurs across the β_i circle, suppose that $\mathcal{G}_2$ has the same horizontal circles, $\boldsymbol{\alpha}$, and has vertical circles given by $\boldsymbol{\gamma} = \{\beta_1, ..., \beta_{i-1}, \gamma_i, \beta_{i+1}, ..., \beta_n\}$. In the modified grid diagram, draw the vertical circles so

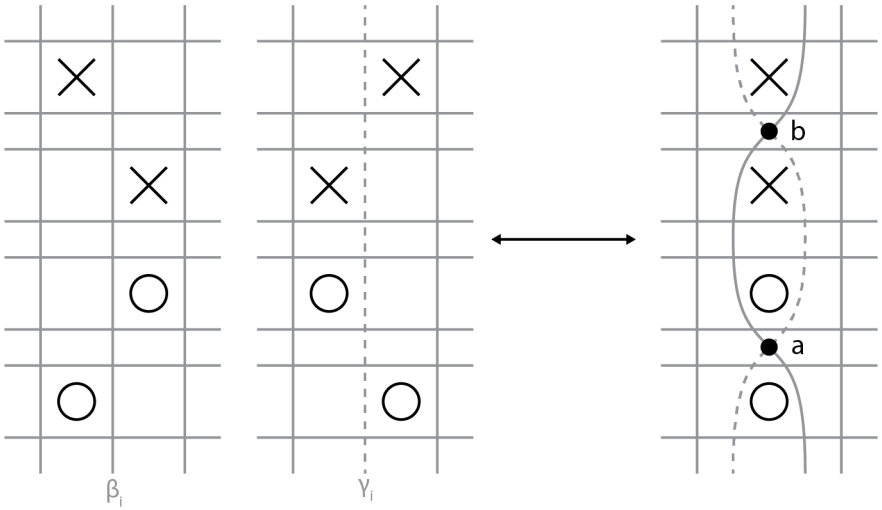

Figure 9: Commutation Diagram

that β_i and γ_i meet perpendicularly at two points that are not along horizontal circles. One of the two intersection points will be at the bottom of the bigon whose leftmost boundary is β_i and rightmost boundary is γ_i, label this intersection point as a and the other as b. This construction can be seen in Figure 9.

For grid states $\mathbf{x} \in \mathbf{S}(\mathcal{G}_1)$ and $\mathbf{y}' \in \mathbf{S}(\mathcal{G}_2)$, a *pentagon* p from $\mathbf{x}$ to $\mathbf{y}'$ is an embedded disk in the torus where

- $\partial p \subseteq \gamma_i \cup \bigcup_{i=1}^{n} \alpha_i \cup \beta_i$ and consists of five arcs.
- Four of the corners of p are in $\mathbf{x} \cup \mathbf{y}'$.
- At each corner point x, a small disk centered at x is divided into four pieces by the circles forming the circles which are intersecting at the corner point. p contains exactly one of these pieces.
- $\partial(\partial_{\boldsymbol{\alpha}} p) = \mathbf{y}' - \mathbf{x}$.

The set of all pentagons from $\mathbf{x}$ to $\mathbf{y}'$ will be denoted $\mathrm{Pent}(\mathbf{x}, \mathbf{y}')$. A pentagon $p \in \mathrm{Pent}(\mathbf{x}, \mathbf{y}')$ is an *empty pentagon* if $p \cap \mathbf{x} = p \cap \mathbf{y}' = \emptyset$, and the set of all empty pentagons will be denoted $\mathrm{Pent}^{\circ}(\mathbf{x}, \mathbf{y}')$.

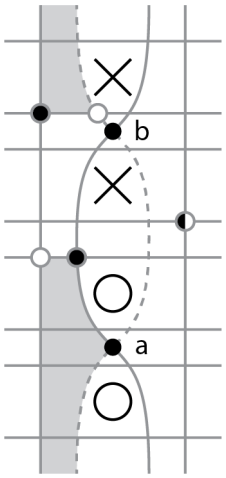

Figure 10: A Pentagon in a Commutation Diagram

Theorem 2.7. *([12], Proposition 3.2) The chain map* $P : GC^-(\mathcal{G}_1) \to GC^-(\mathcal{G}_2)$ *defined on grid states by*

$$P(\mathbf{x}) = \sum_{\mathbf{y}\in\mathbf{S}(\mathcal{G}_2)} \sum_{\{p\in Pent^\circ(\mathbf{x},\mathbf{y}') \,|\, p\cap\mathbb{X}=\emptyset\}} V_1^{\mathcal{O}_1(p)} \cdots V_n^{\mathcal{O}_n(p)} \cdot \mathbf{y}',$$

and extended linearly to all of $GC^-(\mathcal{G}_1)$*, is a quasi-isomorphism.*

By combining this theorem with the relationship between $GC^-(\mathcal{G})$ and $\widehat{GC}(\mathcal{G})$, the homology in either version of grid homology is unchanged under commutation moves.
To show that the homology associated to these chain complexes is a knot invariant, it remains to show that they are invariant under stabilizations as well. Here, we give a brief outline of the argument for stabilizations of types $S : XNW$ and $S : XSE$, as these will be the necessary stabilizations in the Legendrian setting. The other stabilizations can be shown to produce isomorphic grid homology theories by making a slight modification in the argument we outline here, and the full version of the argument can be seen in either [19] or [12].
Let $\mathcal{G}_2$ be a grid diagram obtained from $\mathcal{G}_1$ by a stabilization. Since stabilizing not only changes the grid size, but also the number of O-markings, and thus the base ring, we need to decompose both $GC^-(\mathcal{G}_2)$ and ∂^- into pieces which will be either trivial in homology or

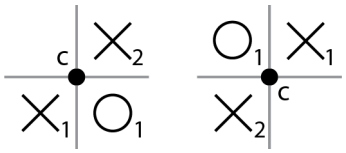

Figure 11: Labelings in an $S : XNW$ Stabilization (left) and an $S : XSE$ Stabilization (right)

equivalent to $GC^-(\mathcal{G}_1)$.

For a stabilization of type $S : XNW$, number the X and O markings so that O_1 is the newly introduced O marking, X_1 is to the left of O_1, and X_2 is above O_1. For a stabilization of type $S : XSE$, number the X and O markings so that O_1 is the newly introduced O marking, X_1 is to the right of O_1 and X_2 is below O_1 (both $S : XNW$ and $S : XSE$ are pictured in Figure 11). Let c denote the intersection point of the newly added circles in the grid. Moreover, $\mathbf{S}(\mathcal{G}_2)$ can be decomposed into $\mathbf{I}(\mathcal{G}_2) \cup \mathbf{N}(\mathcal{G}_2)$ where $\mathbf{I}(\mathcal{G}_2)$ consists of the grid states that contains c as one of their points, and $\mathbf{N}(\mathcal{G}_2)$ is the grid states that do not contain c. In fact, this decomposition gives a splitting of $GC^-(\mathcal{G}_2) = \mathbf{I} \oplus \mathbf{N}$, where $\mathbf{I}$ is a subcomplex, as any rectangle $r \in \mathrm{Rect}(\mathbf{x}, \mathbf{y})$ with $\mathbf{x} \in \mathbf{I}(\mathcal{G}_2)$ and $\mathbf{y} \in \mathbf{N}(\mathcal{G}_2)$ must contain an X marking. This decomposition of $GC^-(\mathcal{G}_2)$ gives a decomposition of ∂^- as

$$\partial^- = \begin{pmatrix} \partial^{\mathbf{I}}_{\mathbf{I}} & \partial^{\mathbf{I}}_{\mathbf{N}} \\ 0 & \partial^{\mathbf{N}}_{\mathbf{N}} \end{pmatrix}.$$

Let $\mathbf{I}$ be the free $\mathcal{R}$-module generated by $\mathbf{I}(\mathcal{G}_2)$. The one-to-one correspondence between $\mathbf{S}(\mathcal{G}_1)$ and $\mathbf{I}(\mathcal{G}_2)$ gives an isomorphism, $e : \mathbf{I} \to GC^-(\mathcal{G}_1)[V_1]$.

Proposition 2.8. *([12], Proposition 3.8) Suppose $\mathcal{G}_2$ is obtained from $\mathcal{G}_1$ by a stabilization of type $S : XNW$ or $S : XSE$. Then there is an isomorphism from $GH^-(\mathcal{G}_2) \cong GH^-(\mathcal{G}_1)$ whose restriction to $\mathbf{I}$ is the map on homology induced by e followed by a projection π.*

The main idea of the proof is to use e, its inverse e^{-1}, and a chain homotopy equivalence

$\mathcal{H} : \mathbf{I} \to \mathbf{N}$ defined by

$$\mathcal{H}(\mathbf{x}) = \sum_{\mathbf{y} \in \mathbf{N}(\mathcal{G}_2)} \sum_{\{r \in \mathrm{Rect}^\circ(\mathbf{x},\mathbf{y}) \,|\, \mathrm{Int}(r) \cap \mathbb{X} = X_2\}} V_1^{\mathcal{O}_1(r)} \cdots V_n^{\mathcal{O}_n(r)} \cdot \mathbf{y}.$$

to set up the square

$$\begin{array}{ccc} \mathbf{N} & \xrightarrow{\partial^{\mathbf{I}}_{\mathbf{N}}} & \mathbf{I} \\ {\scriptstyle \mathcal{H} \circ e^{-1}} \uparrow & & \uparrow {\scriptstyle e^{-1}} \\ GC^-(\mathcal{G}_1)[V_1] & \xrightarrow{V_1 - V_2} & GC^-(\mathcal{G}_1)[V_1] \end{array}$$

which commutes as is shown in [12].

From homological algebra, such a square induces a quasi-isomorphsim

$\Phi : \mathrm{Cone}(V_1 - V_2) \to GC^-(\mathcal{G}_2)$, where $\mathrm{Cone}(V_1 - V_2)$ is the homological mapping cone of the chain map $V_1 - V_2 : GC^-(\mathcal{G}_1)[V_1] \to GC^-(\mathcal{G}_1)[V_1]$. The induced maps on homology give a commutative square

$$\begin{array}{ccc} H(\mathbf{I}) & \longrightarrow & GH^-(\mathcal{G}_2) \\ {\scriptstyle H(e^{-1})} \uparrow & & \uparrow {\scriptstyle H(\Phi)} \\ GH^-(\mathcal{G})[V_1] & \xrightarrow{\pi} & H(\mathrm{Cone}(V_1 - V_2)) \end{array} ,$$

since $H(\mathrm{Cone}(V_1 - V_2)) \cong GH^-(\mathcal{G}_1)$. $H(\Phi)$ is an isomorphism, so the proposition holds.

The above theorem shows invariance for stabilizations of types $S : XNW$ and $S : XSE$. As mentioned earlier, slight modification of the argument can be used to show invariance for $S : XNE$ and $S : XSW$, or one can adapt the commutation moves to a specialized move called a switch, which can be used to change a stabilization of type $S : XNW$ into any X stabilization.

2.6 Collapsed and Uncollapsed Grid Homology for Links

Let L be a link with l components, and let $O_{j_1}, ..., O_{j_l}$ be O markings which are on the l different components of L. The collapsed grid chain complex associated to $\mathcal{G}$ is the chain

complex $cGC^-(\mathcal{G}) = \dfrac{GC^-(\mathcal{G})}{V_{j_1} = \cdots = V_{j_l}}$. The homology of this chain complex is the collapsed grid homology associated to $\mathcal{G}$. The fact that this homology is an invariant of the underlying link follows from straightforward adaptations of the ideas from the 2.5 along with an adaptation of Lemma 2.6.

The uncollapsed grid homology for links is also defined in an analogous way to the grid homology for knots, but instead of identifying variables coming from different components of the link, extra structure is given to the underlying polynomial ring. For a grid $\mathcal{G}$ representing a link L with l components, the uncollapsed grid homology is the homology of the chain complex $GC^-(\mathcal{G})$ thought of as a module over $\mathbb{Z}_2[U_1, ..., U_l]$ where the action of U_i is multiplication by V_{j_i}, where O_{j_i} corresponds to an O marking on the ith component of L.

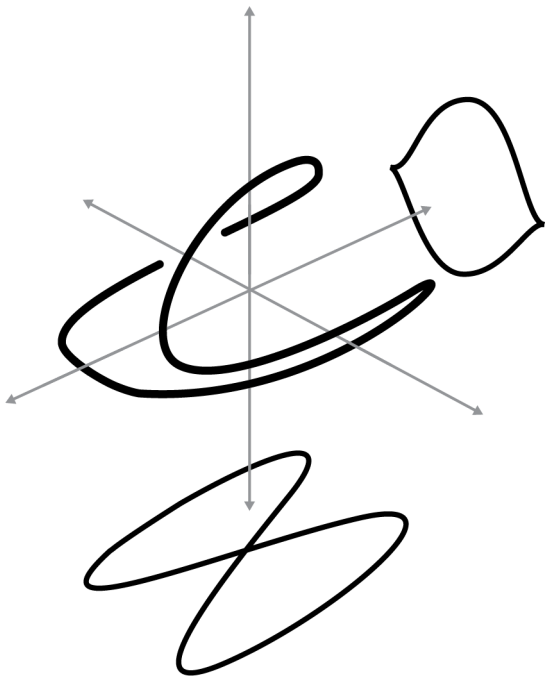

Figure 12: Front and Lagrangian Projections of a Legendrian Unknot

3 Legendrian Links

This section gives a brief discourse on the contact geometry necessary for understanding Legendrian links in our setting. For a more thorough exposition on symplectic and contact geometry, see [13], or if just interested in more information regarding Legendrian links, see [7]. Let M be a 3-manifold and ξ a non-integrable plane field in TM. Locally ξ can be described as the kernel of $\alpha \in \Omega^1(M)$. ξ is a contact structure on M if $\alpha \wedge d\alpha \neq 0$. For $\mathbb{R}^3$, the *standard contact structure* is given by $\ker(\alpha_0) = \ker(dz - ydx)$. The following theorem shows that this standard contact manifold is the only local model for contact manifolds.

Theorem 3.1. *(Darboux, Moser, [14]) If (M, ξ) is a contact 3-manifold, and near a point $a \in M$, $\xi = \ker(\alpha)$, then there is a local coordinate system near a, (x_1, x_2, x_3), so that $\alpha = dx_3 - x_2 dx_1$. That is, (M, ξ) locally looks like the standard contact manifold $(\mathbb{R}^3, \xi_0)$.*

A *Legendrian link* Λ in a contact manifold (M, ξ) is a link in M where $T_x\Lambda \subseteq \xi_x$. We will restrict to the case of Legendrian links the standard contact $(\mathbb{R}^3, \xi_0)$.

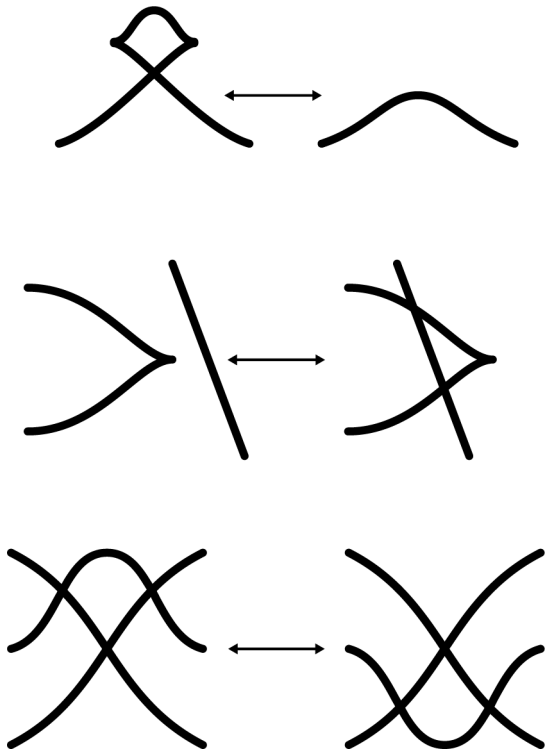

Figure 13: Front Projection Reidemeister Moves LRM1 (top), LRM2 (middle), and LRM3 (bottom)

3.1 Diagrams of Legendrian Links

There are two projections which are commonly used when creating link diagrams for Legendrian links - the front projection and the Lagrangian projection.

The *front projection* is the projection $\pi_y : \mathbb{R}^3 \to \mathbb{R}^2$ defined by $\pi_y(x, y, z) = (x, z)$, and the image $\pi_y(\Lambda)$ is the front projection of Λ. Notice that since $\xi_0 = \ker(dz - ydx)$, if $s : [0, 1] \to \mathbb{R}^3$ is a parametrization of Λ, then $z'(s) - y(s)x'(s) = 0$, and so $y(s) = \dfrac{z'(s)}{x'(s)}$. Thus, at a point $a \in \pi_y(\Lambda)$, the y-coordinate of Λ can be recovered from $\pi_y(\Lambda)$ by considering the slope of Λ at a.

The contact structure gives the front projection a three defining features, which are based on the fact that the y-coordinate can be recovered by the slope,

1. $\pi_y(\Lambda)$ will have no vertical tangencies.

2. The only places where π_y fails to be an immersion are at cusps.

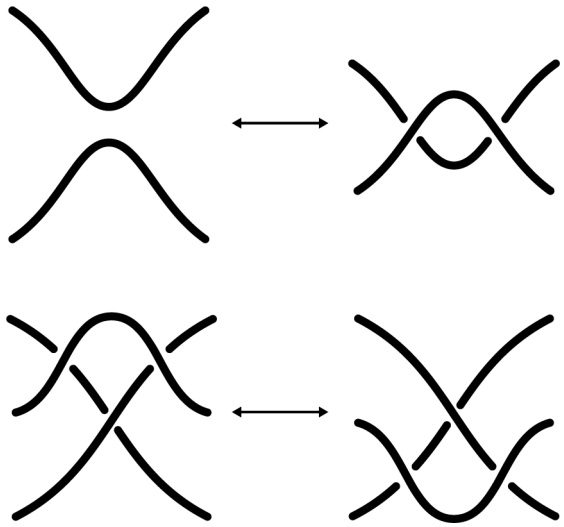

Figure 14: Lagrangian Projection Reidemeister Moves

3. At double points of $\pi_y(\Lambda)$, the slope of the overcrossing is smaller than the slope of the undercrossing.

The following theorem gives a correspondence between Legendrian isotopy and moves on front diagrams,

Theorem 3.2. *([28]) Two front diagrams represent Legendrian isotopic Legendrian links if and only if they are related by a sequence of planar isotopies that do not introduce vertical tangenices and Legendrian front Reidemeister moves.*

The *Lagrangian projection* is the projection $\pi_z : \mathbb{R}^3 \to \mathbb{R}^2$ defined by $\pi_z(x, y, z) = (x, y)$, and the image $\pi_z(\Lambda)$ is the Lagrangian projection of Λ. When using the Lagrangian projection, the original Legendrian can be recovered from $\pi_z(\Lambda)$ up to a vertical translation, as $z(s) = z_0 + \int_0^s x'(t)y(t)dt$.
Unlike the front projection, this projection has only a weak version of the Reidemeister theorem, where Legendrian links may be related by additional moves than just those in Figure 14,

Proposition 3.3. *([7], Theorem 2.8) If two Lagrangian link diagrams are related by a*

sequence of Lagrangian Reidemeister moves then they represent Legendrian isotopic Legendrian links.

3.2 Classical Legendrian Invariants

Given a Legendrian link Λ, there are three classical invariants which are used to distinguish their Legendrian isotopy classes. The first of these classical invariants is the underlying topological link type. Any Legendrian link is also a topological link, and any Legendrian isotopy between links is also a smooth isotopy. Thus, if two Legendrians have different topological link types then they have different Legendrian link types.

The second of the classical invariants is the Thurston-Bennequin number. While this invariant has many equivalent definitions, we will primarily use the definition which is based off of a front diagram of Λ. Given the front projection $\pi_y(\Lambda)$ of Λ, let $U(\Lambda)$ denote the number of upwards oriented cusps and let $D(\Lambda)$ denote the number of downwards oriented cusps. The *Thurston-Bennequin number* is defined to be $tb(\Lambda) = \text{wr}(\Lambda) - \frac{1}{2}(U(\Lambda) + D(\Lambda))$ where $\text{wr}(\Lambda)$ denotes the writhe of the diagram.

The final classical invariant is the *rotation number*. Again, using the front diagram, this can be defined as $r(\Lambda) = \frac{1}{2}(D(\Lambda) - U(\Lambda))$.

While it is now known that these three invariants alone do not distinguish all Legendrian isotopy classes of Legendrian links, they are able to differentiate many classes. A topological link L where all Legendrian links representing L are determined by their Thurston-Bennequin number and rotation number are called *Legendrian simple*. In fact, the first Legendrian non-simple knot is $m(5_2)$, of which, the two different Legendrian can be distinguished using the Legendrian grid invariants, ruling invariants, and linearized contact homology.

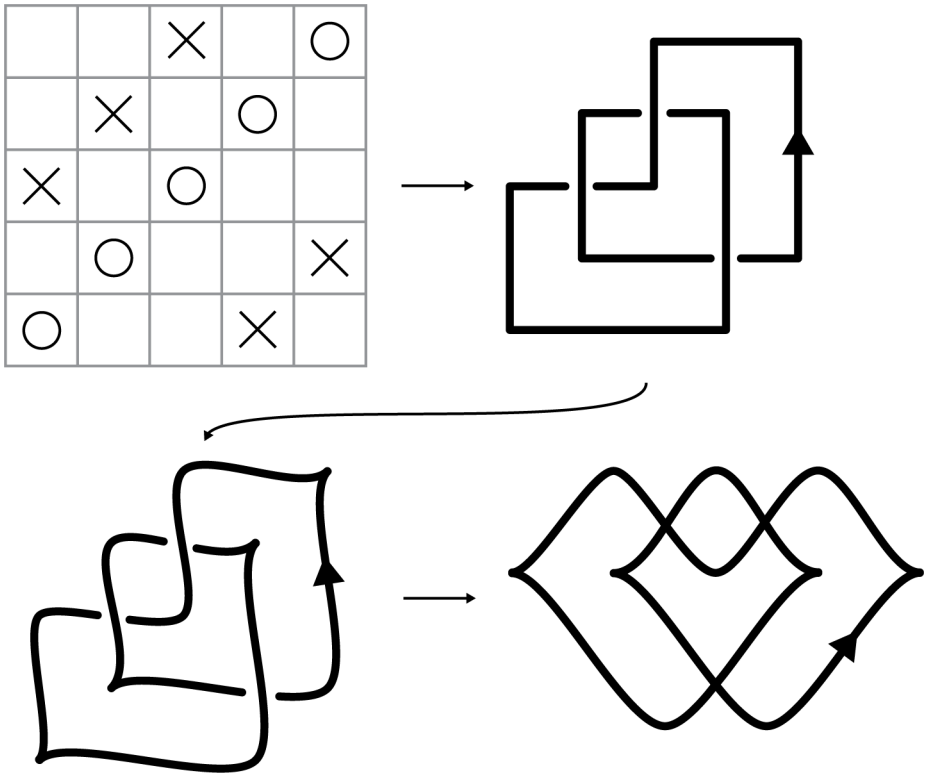

Figure 15: Association of a Grid Diagram and a Legendrian Link

3.3 Grid Diagrams and Legendrian Links

Grid diagrams represent Legendrian links in a natural way. To obtain the front diagram for a Legendrian link from a grid diagram $\mathcal{G}$,

1. let L be the piecewise-linear link specified by $\mathcal{G}$,
2. smooth out any NW or SE corners of the diagram,
3. turn any NE or SW corners of the diagram into cusps,
4. rotate the diagram 45° clockwise,
5. reverse all crossings so that they match the front diagram requirements on the slope.

Just as in the case of oriented links, every Legendrian link can be represented by a grid diagram. The crossing information is already correct, as the slope condition on the strands

guarantees this. Stretch the front diagram horizontally until no part of the link forms an angle of more than 45° to the horizon. Reversing the procedure in Figure 15 gives a grid diagram associated to Λ.

In fact, not only do grid diagrams relate to Legendrian links via the front diagram in a natural way, a subcollection of grid moves is able to give a Reidemesiter-type theorem for grids representing Legendrians.

Theorem 3.4. *([24], Proposition 4.4) Two grid diagrams represent Legendrian isotopic Legendrian links if and only if the grid diagrams are related by a sequence of commutation moves or stabilizations and destabilizations of type $(S : XNW)$, $(S : XSE)$, $(S : ONW)$, and $(S : OSE)$.*

With the relationship between X and O stabilizations presented in Proposition 2.4., the above theorem can in fact be reduced to only considering the two types of X stabilizations. Moreover, the proof of the equivalence of cyclic permutations only uses the allowed grid moves for Legendrian links. Thus, cyclic permutations correspond to diagrams of Legendrian isotopic links.

3.4 Legendrian Grid Invariants from Grid Homology

For a grid diagram $\mathcal{G}$, let $\mathbf{x}^+$ and $\mathbf{x}^-$ be the two grid states whose components are the northeast and southwest corners, respectively, of squares with X markings of $\mathcal{G}$. Notice that any rectangle from $\mathbf{x}^\pm$ will necessarily contain an X marking, and so in any of the three discussed homology theories these grid states represent cycles, as none of the differentials count rectangles which contain an X marking. Let $\lambda^\pm(\mathcal{G})$ be the homology classes of $\mathbf{x}^\pm$ in $\mathcal{G}$, respectively.

Theorem 3.5. *([24], Theorem 1.1) Let $\mathcal{G}_1$ and $\mathcal{G}_2$ be two grid diagrams that represent Legendrian isotopic knots. There is an isomorphism $\phi : GH^-(\mathcal{G}_1) \to GH^-(\mathcal{G}_2)$ where $\phi(\lambda^\pm(\mathcal{G}_1)) = \lambda^\pm(\mathcal{G}_2)$.*

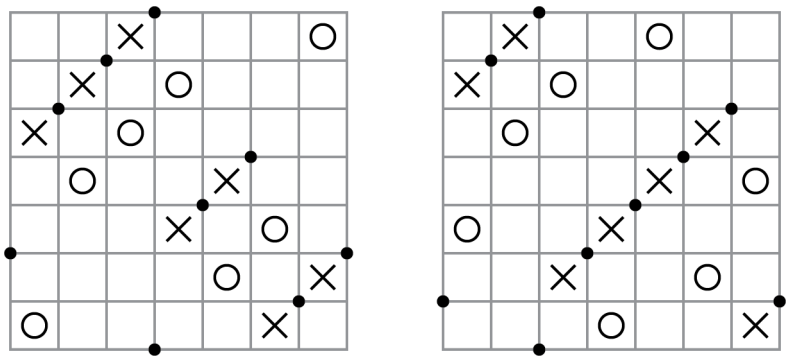

Figure 16: Legendrian Non-simple $m(5_2)$ Knots with $\mathbf{x}^+$

While computing $\lambda^{\pm}(\mathcal{G}_1)$ directly can be difficult and require computer assistance, it is possible to distinguish Legendrian links by determining if $\lambda^{\pm}(\mathcal{G}_1)$ are zero or nonzero, or by determining if $\lambda^+(\mathcal{G}_1) = \lambda^-(\mathcal{G}_1)$ or if $\lambda^+(\mathcal{G}_1) \neq \lambda^-(\mathcal{G}_1)$. Chekanov in [5] used linearized contact homology to show that $m(5_2)$ with $tb = 1$ and $r = 0$ are Legendrian non-simple knots, but these can also be distinguished using $\lambda^{\pm}$. Grid diagram representations of the two Legendrian knots, with $\mathbf{x}^+$, are pictured in Figure 16.

Corollary 3.6. *If $\mathcal{G}_1$ and $\mathcal{G}_2$ are two grid diagrams that represent Legendrian isotopic knots, then there is an isomorphism $\widehat{\phi} : \widehat{GH}(\mathcal{G}_1) \to \widehat{GH}(\mathcal{G}_2)$ where $\phi(\widehat{\lambda}^{\pm}(\mathcal{G}_1)) = \widehat{\lambda}^{\pm}(\mathcal{G}_2)$, where $\widehat{\lambda}^{\pm}$ is the homology class of $\mathbf{x}^{\pm}$ in $\widehat{GH}$.*

The above corollary follows, by comparing the differentials from GH^- and $\widehat{GH}$. Notice here that the differential in $\widehat{GH}$ is a restriction of the differential in GH^-.
While in general $\widehat{GH}$ has less algebraic structure than GH^-, more often it is easier to compute $\widehat{\lambda}^{\pm}$ instead of $\lambda^{\pm}$. In fact, the connection between $\widehat{GH}$ and $\widetilde{GH}$ provides information about $\widehat{\lambda}^{\pm}$. Notice that $\widehat{\lambda}^{\pm} = 0$ if and only if $\mathbf{x}^{\pm}$ represents the trivial homology class in $\widetilde{GH}$.

4 Singular Links and Allowable Singular Grid Diagrams

Singular knots and links arise not only as a direct generalization of knot theory, but are crucial components of understanding Vassiliev invaraints. In particular, singular links appear in the Vassiliev Skein relation, where the singularity is resolved to be either a positive or negative crossing. Due to this relation, many Vassiliev link invariants extend to singular links via this Skein relation. Moreover, Skein relations involving singular knots and links are the focus of the singular grid diagram construction presented in [29].
In the Legendrian setting, singular Legendrian links can be used to further understand Giroux open books. The classical Legendrian invariants (the Thurston-Bennequin and rotation numbers) also have generalizations to the singular Legendrian setting, as explored in [1]. To this end, it would be interesting to use the singular grid invariants defined here to discover isotopic singular non-simple Legendrian links.

4.1 Singular Links

A *regular double point* of an immersion $f : S^1 \to \mathbb{R}^3$ is a point $p \in \mathbb{R}^3$ where two points $x_1 \neq x_2$ in S^1 with $f(x_1) = f(x_2) = p$ satisfy $\operatorname{codim}\left(T_{x_1}\left(f(S^1)\right) + T_{x_2}\left(f(S^1)\right)\right) = 1$. A *singular link* S is an immersion $\coprod_{i=1}^{n} S^1 \to \mathbb{R}^3$, with finitely many regular double points, which are often referred to as the *singular points* of S. Just as with nonsingular links, we consider singular links up to ambient isotopy.
We can construct a diagram representing S by taking a generic orthogonal projection onto a plane in $\mathbb{R}^3$. This projection, since generic, is assumed to be an immersion everywhere except at points which are projected from the singular points. As singular points are regular double points, it is generic to require that, in the projection, the strands forming a singular point intersect transversely at the singular point.
To relate singular links to singular link diagrams, we have the following theorem which translates ambient isotopy of singular links to a set of moves on singular diagrams,

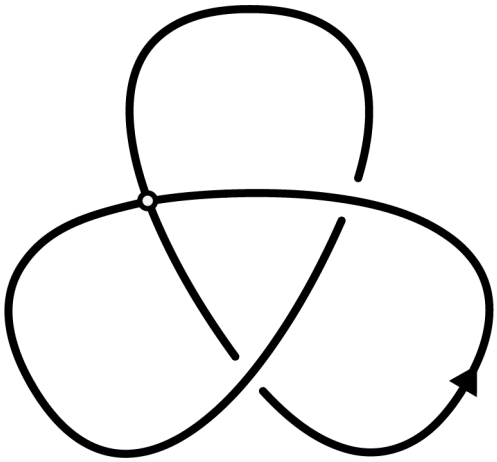

Figure 17: Oriented Singular Link Diagram

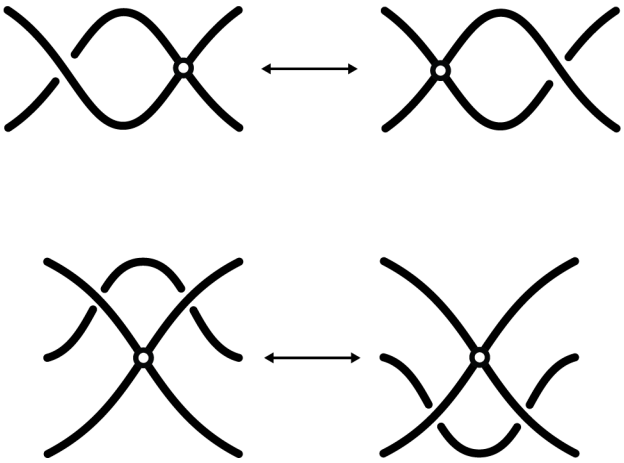

Figure 18: Singular Reidemeister Moves

Theorem 4.1. *(Kauffman, [9]) Two singular links diagrams represent ambient isotopic singular links if and only the diagrams are related by a finite sequence of planar isotopies, Reidemeister moves, or singular Reidemeister moves.*

For labeling purposes, the first move depicted in Figure 18 will be called a singular flype move (SF), and the second will be called a singular Reidemesiter 3 move ($SRM3$). As before, these two moves generate the full collection of singular Reidemeister moves by allowing rotations, mirroring, and a consistent change in crossings in the local models.

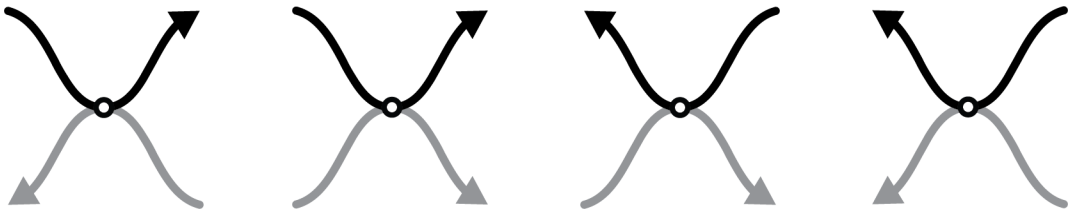

Figure 19: Orientations Near a Singularity for a Singular Legendrian

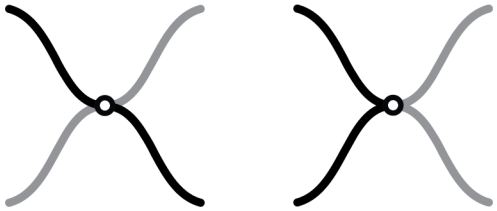

Figure 20: Invalid Strand Configurations Near a Singularity

4.2 Singular Legendrian Links

A *singular Legendrian link* Λ^* is a singular link that is Legendrian with respect to the standard contact $(\mathbb{R}^3, \xi_0)$. We can obtain the front diagram and Lagrangian diagram as before, by taking the projections onto the xz- and xy-planes, respectively.

Notice that in the front diagram of Λ^*, the projection does not satisfy the generic condition on projections, as any singularity must be a nontransverse intersection in the diagram. This is the case because the slope of the strands near the singularity must be the same, otherwise it would not correspond to an intersection in $\mathbb{R}^3$.

There are many possible local models for singular points in link diagrams which are non-transverse intersections. By considering the Lagrangian projection as well, in order to have an intersection in the front diagram which comes from a singular point of Λ^*, there are only four possible local models, as seen in Figure 19, that can occur near a singular point. Notice that in these models, the strands are colored differently, to keep track of how the singularity is formed. Some invalid strand configurations can be seen in Figure 20.

Just as before, in order define invariants of singular Legendrian links, we need to implement a Reidemeister-type theorem for front diagrams of singular Legendrian links. As

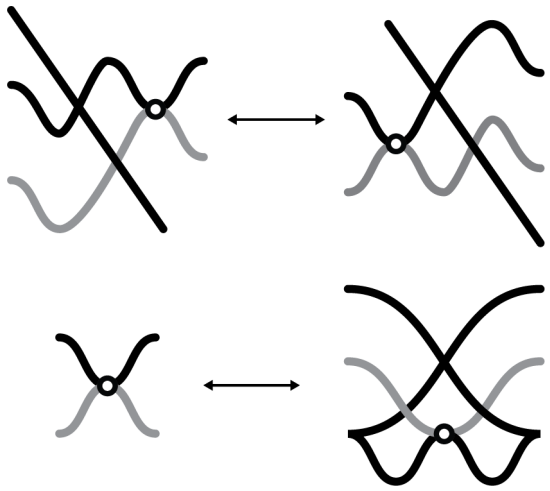

Figure 21: Singular Legendrian Reidemeister Moves $SLRM1$ (top) and $SLRM2$ (bottom)

was done in [1], an adaptation of a Reidemeister theorem for graphs, as presented in [4], gives the following theorem,

Theorem 4.2. *([4], [1]) Two singular Legendrian front diagrams represent Legendrian isotopic singular Legendrian links if and only if the singular front diagrams are related by a sequence of planar isotopies which do not introduce vertical tangencies, Legendrian Reidemeister moves ($LRM1$, $LRM2$, or $LRM3$), or singular Reidemeister moves ($SLRM1$ and $SLRM2$).*

The two generating singular Legendrian Reidemeister moves are pictured in Figure 21.

4.3 Singular Grid Diagrams

In this section, we first recall the construction given in [8] with slight modifications that will be useful in our setting. Notice that in the setting of [8], the singular grid diagrams have a natural association to a class of graphs, and thus is more general that what we need for our purposes.

A *singular grid diagram* $\mathcal{G}^*$ is an $(n \times n)$ grid in the plane along with a set of n X markings $\mathbb{X}$ and a set of m O markings $\mathbb{O}$, where $m \geq n$, so that the rules below hold.

- Each row and column contains exactly one X marking.

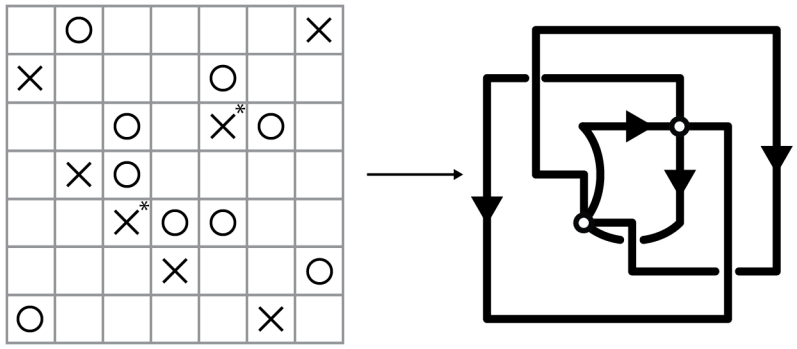

Figure 22: A Singular Grid Diagram and its Corresponding Graph

- Each row and column may have either one or two O markings. Any X marking in the same row or column as two O markings will be decorated with an $*$.
- If there is an X^* marking in the (i, j)th square, both R_i and C_j have two O markings.
- A square in the grid contains at most one marking.

To each singular grid diagram, there is a naturally associated quadrivalent graph, as shown in Figure 22. We use the convention that, in columns which correspond to a singularity, if the O markings are entirely above or below the X^* marking, that the strand connecting the O marking furthest from the X^* marking curves to the right. Similarly, for rows, we use the convention that the strand connecting the O marking furthest from the X^* marking curves downwards.

These rules, however, are not enough to ensure that a singular grid diagram directly specifies a singular Legendrian front diagram. Also as seen in Figure 22, the natural description of a graph coming from a singular grid diagram does not necessarily fit any of the four local models for singularities in a front diagram of Figure 19. To resolve this issue we take the following steps, which will be described in more detail over the next few sections,

1. restrict to a subcollection of singular grid diagrams, which we will call allowable singular grid diagrams,

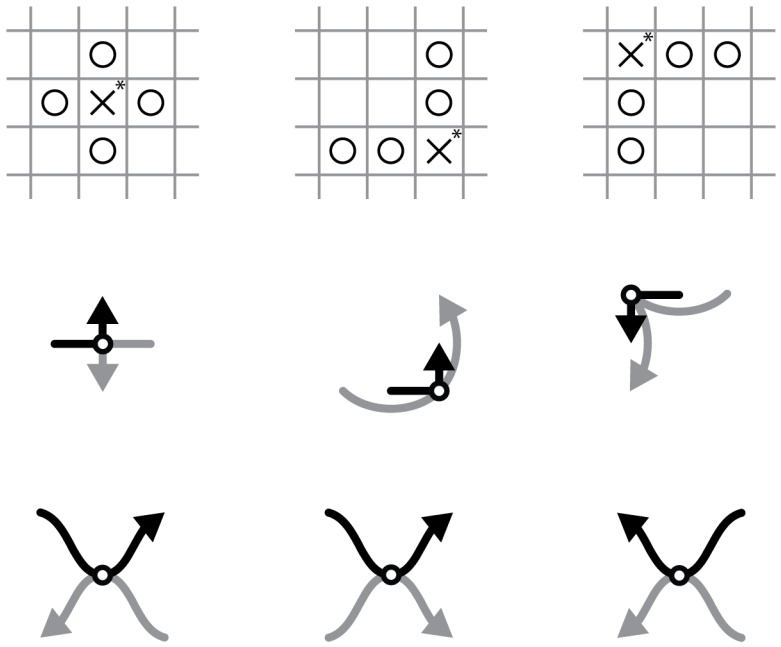

Figure 23: Allowable Grid Configurations Near Singularities

2. show that an allowable singular grid diagram specifies a singular *Legendrian* front diagram,

3. describe grid moves which allow us to transition between singular Legendrian front diagrams.

4.4 Allowable Singular Grid Diagrams

For a given singular grid diagram $\mathcal{G}^*$, to describe the singular Legendrian front diagram associated to it, we follow the same steps as in Figure 15, where we modify the graph described by $\mathcal{G}^*$ by rotating the diagram, switch the crossings, and changing the corners into cusps or smoothing them out. As seen in the last section, in this more general graph setting, this process does not always describe a singular Legendrian front diagram. To remedy this, we restrict the possible configurations for a singular grid diagram in the rows and columns corresponding to a singularity.

To discover the proper restriction of the class of singular grid diagrams, consider the

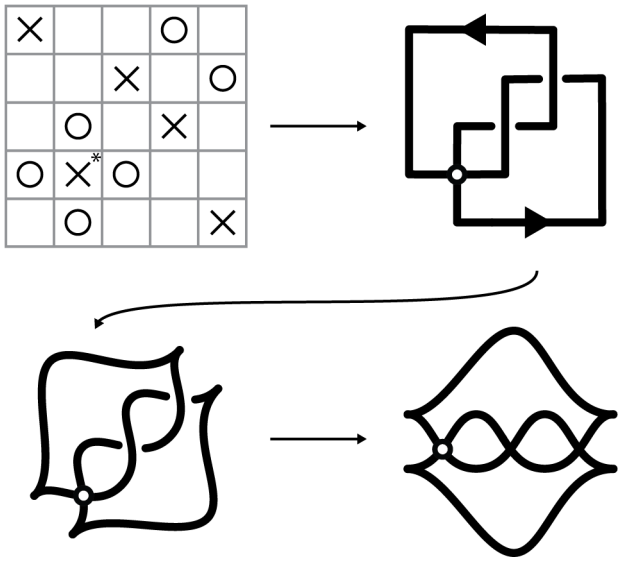

Figure 24: Allowable Singular Grid Diagram and its Corresponding Singular Legendrian Front Diagram

possible local models for the singular grid diagram. Notice that if we desire to transition the associated graph into a singular Legendrian front diagram, the only local models which follow the orientation models near a singularity in a singular Legendrian front diagram, as in Figure 19, are the grid models pictured in Figure 23.

An *allowable singular grid diagram* is a singular grid diagram where the only configurations of singular rows and columns are the ones in Figure 23, with possibly extra rows/columns inserted between the markings. As described previously, every allowable singular grid diagram has an associated singular Legendrian front diagram. The correspondence in this setting is pictured in Figure 24.

In fact, every singular Legendrian front diagram Λ^* has a singular grid diagram $\mathcal{G}^*$ for which the singular Legendrian front diagram associated to $\mathcal{G}^*$ can be related to Λ^* by applying a necessary amount of $SLRM2$ moves. To construct such a diagram, notice that the local models in consideration in Figure 23 have an orientation that is forced by the grid. It, therefore, remains to show that there is an allowable singular grid model for any orientation near the singularity. All cases are shown in Figure 25.

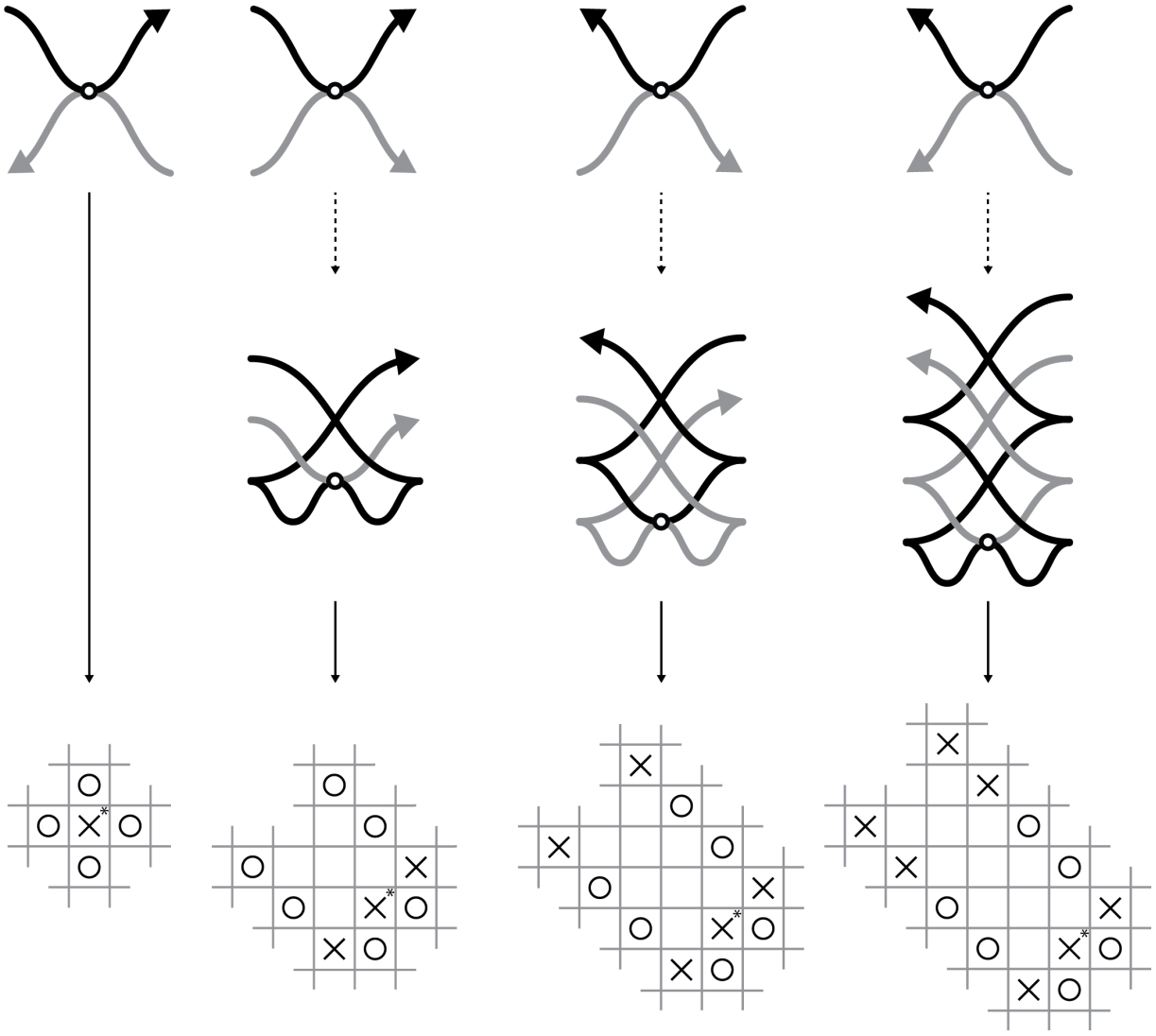

Figure 25: Local Singular Grid Diagram for a Singular Legendrian Fronts Near a Singularity

5 Singular Grid Moves

To develop a singular grid homology theory that is an invariant for singular Legendrian links, we need to adapt the grid moves for nonsingular grid diagrams so that the grid moves can be applied near a singular point. Before defining these singular grid moves, we assume that all nonsingular grid moves can still be applied, as long as they are not interacting with a X^* marking or any O markings which are in the same row or column as an X^* marking. In this section, we will define the moves used in [8] for our modification, and so they will be moves for singular grid diagrams which represent graphs. After defining the full collection of moves, we then restrict this class of moves to the ones necessary for singular Legendrian Reidemeister moves. A comparison between the moves used for allowable singular grid diagrams and graph grid diagrams in [8] will be discussed in section 6.

5.1 Singular Commutations

Let $\mathcal{G}_1^*$ be a singular grid diagram and let C_i and C_{i+1} be two consecutive columns in $\mathcal{G}^*$, one of which contains an X^* marking and the other of which does not contain an X^* marking. Suppose C_i contains the X^* marking. Let $I_1, I_2 \subseteq \mathbb{R}$ denote the two closed intervals whose endpoints correspond to the vertical positions of the two O markings and X^* marking in C_i, and let $I_i = I_1 \cup I_2$. Let $I_{i+1} \subseteq \mathbb{R}$ denote the closed interval whose endpoints correspond to the vertical positions of the X and O markings in C_{i+1}. A *type 1 singular column commutation* of $\mathcal{G}_1^*$ into a new singular grid diagram $\mathcal{G}_2^*$ is obtained by swapping the consecutive columns C_i and C_{i+1} provided one of the following holds,

- $I_i \cap I_{i+1} = \emptyset$
- $I_i \subseteq \text{Int}(I_{i+1})$
- $I_1 \subseteq I_2$ or $I_2 \subseteq I_1$, and $I_{i+1} \subseteq \text{Int}(I_1 \cap I_2)$
- $\text{Int}(I_1) \cap \text{Int}(I_2) = \emptyset$ and either $I_{i+1} \subseteq \text{Int}(I_1)$ or $I_{i+1} \subseteq \text{Int}(I_2)$

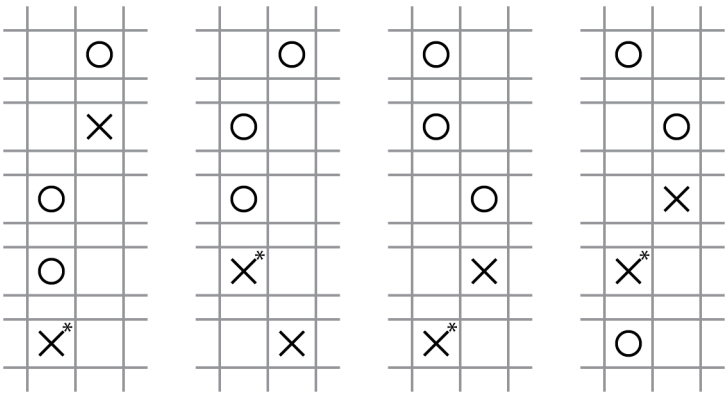

Figure 26: Various Initial Configurations for $C1^*$

The different situations where a type 1 singular column commutation could be applied are pictured in Figure 26. This can be defined analogously for rows, and applying either a type 1 singular column commutation or type 1 singular row commutation will be referred to as a *type 1 singular commutation* and will be labeled as $(C1^*)$.

For the second type of singular commutation, let $\mathcal{G}_1^*$ be a singular grid diagram and let C_i and C_{i+1} be two consecutive columns in $\mathcal{G}_1^*$ which both contain no X^* markings and where the O marking of C_i is in the same row as an X^* marking. As before, let $I_i, I_{i+1} \subseteq \mathbb{R}$ be the closed intervals whose endpoints correspond to the vertical positions of the X and O markings in the columns C_i and C_{i+1}, respectively. A *type 2 singular column commutation* of $\mathcal{G}_1^*$ into a new allowable singular grid diagram $\mathcal{G}_2^*$ is obtained by swapping the consecutive columns C_i and C_{i+1}, provided $I_i \cap I_{i+1} = \emptyset$. Notice that this move does not allow for columns which both contain an O marking in the same row to be swapped. This move can also be defined for rows, and applying either a type 2 singular column commutation or a type 2 singular row commutation will be referred to as a *type 2 singular commutation* and will be labeled as $(C2^*)$. Two situations where a $C2^*$ move can be applied are pictured in Figure 27, in which the leftmost two columns can be swapped.

For the last type of singular commutation move, let $\mathcal{G}_1^*$ be a singular grid diagram and let C_i and C_{i+1} be two consecutive columns in $\mathcal{G}_1^*$ which both contain no X^* markings and where the O markings of C_i and C_{i+1} occur in the same row. This implies that these two O

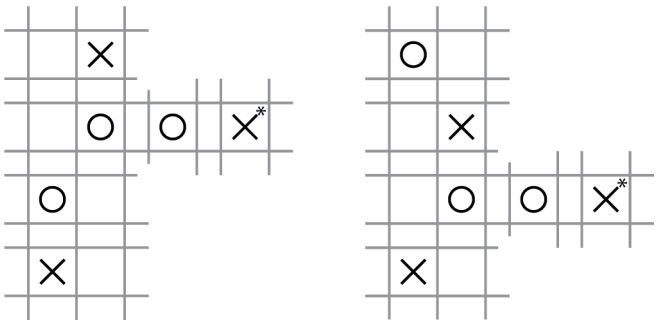

Figure 27: Various Initial Configurations for C2*

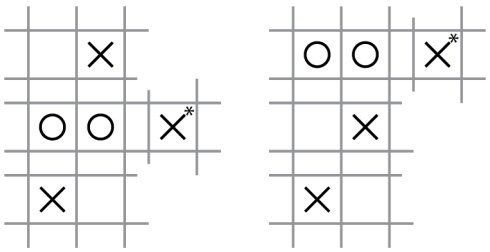

Figure 28: Initial Configuration for $C3^*$

markings are in the same row as an X^* marking. A *type 3 singular column commutation* of $\mathcal{G}_1^*$ into a new singular grid diagram $\mathcal{G}_2^*$ is obtained by swapping the consecutive columns C_i and C_{i+1}. Notice that no other conditions are applied to C_i and C_{i+1} other than that their O markings are in the same row. This move can also be defined for rows, and applying either a type 3 singular column commutation or a type 3 singular row commutation will be referred to as a *type 3 singular commutation* and will be labeled as $(C3^*)$. Two grid configurations where this move can be applied are pictured in Figure 28.

5.2 Singular Stabilizations

In addition to singular commutation moves, there are also singular stabilization moves. Unlike in [8], where the stabilizations occur at the markings in the same row/column as a X^* marking, we will allow stabilizations at the X^* marking itself. In conjunction with $C3^*$, these are conventions equivalent, but when in the Legendrian setting later, the distinction between the two will be important, as $C3^*$ moves preserve the graph type, but do not

preserve the singular Legendrian link type.

Let $\mathcal{G}_1^*$ be a allowable singular grid diagram of grid size n and consider a local model near a X^* marking, which occurs in the ith column and jth row. We present here the case when the O markings occur on opposite sites of the X^* marking. The other allowable grid configurations can be defined analogously, or can be put into this position by sufficiently many cyclic permutations.

A new singular grid diagram $\mathcal{G}_2^*$ of grid size $(n+1) \times (n+1)$ is said to be an X^* *column stabilization* or an X^* *row stabilization* of $\mathcal{G}^*$ if it is obtained from $\mathcal{G}_1^*$ in the following way

1. Remove the X^* marking in the (i, j) square, along with the two O markings in the ith column and the two O markings in the jth row.

2. Split the empty row and column into two rows and two columns by adding a vertical and horizontal line.

3. Replace the markings according to one of the four options in Figure 29 for a column stabilization or replace the markings according to one of the four options in Figure 30 for a row stabilization.

For a labeling convention on the type of stabilization used, we following a similar convention as the nonsingular stabilization. The options are $(RS : X^*NW)$, $(RS : X^*NE)$,$(RS : X^*SW)$, $(RS : X^*SE)$ for row stabilizations and $(CS : X^*NW)$, $(CS : X^*NE)$,$(CS : X^*SW)$, $(CS : X^*SE)$ for column stabilizations, where the location of the empty square in the 2×2 box obtained after stabilizing determines if the stabilization is northwest (NW), southwest (SW), northeast (NE), or southeast (SE).

5.3 Singular Legendrian Front Diagrams and Singular Grid Moves

In order to construct a well-defined grid homology theory for singular Legendrian links, we need to give local allowable singular grid models for the additional singular Legendrian

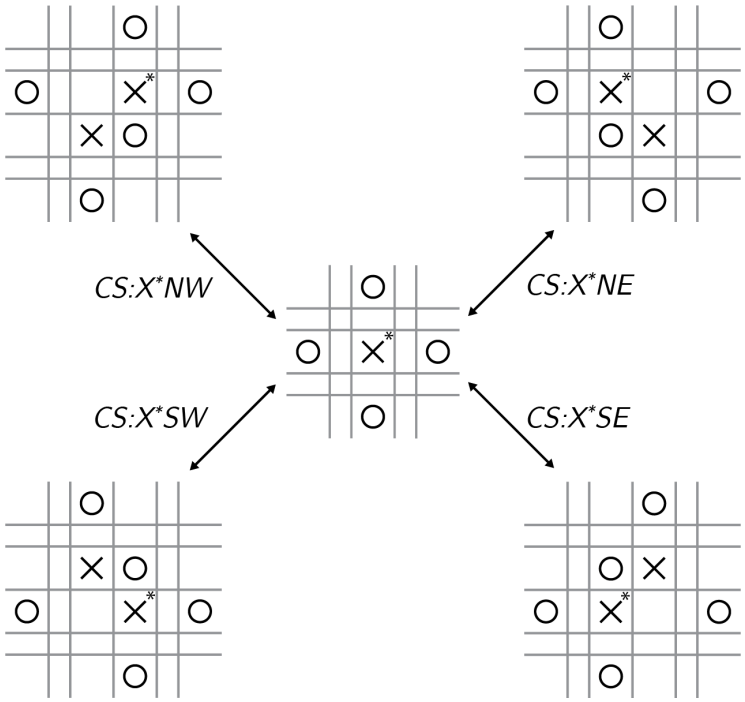

Figure 29: Singular Column Stabilization Configurations

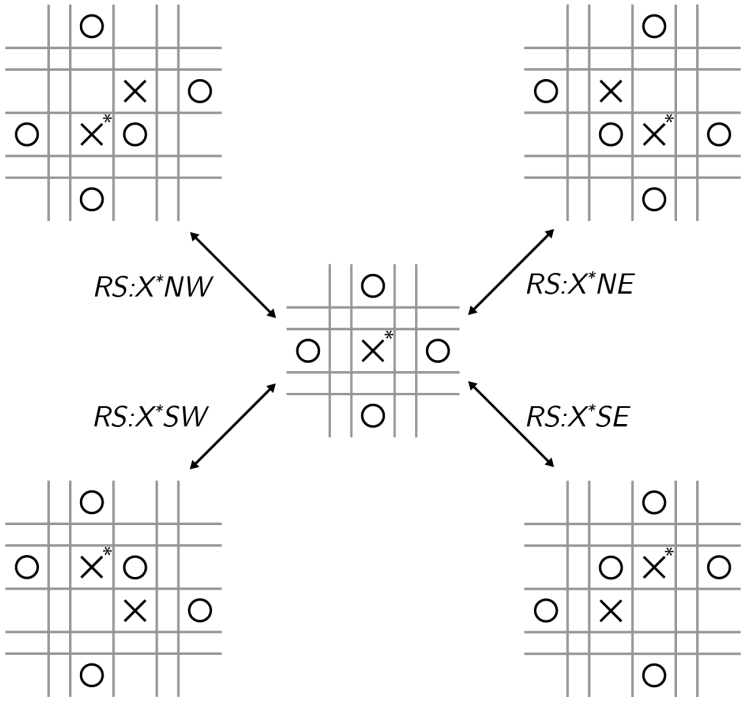

Figure 30: Singular Row Stabilization Configurations

Reidemeister moves, and show that there is a sequence of singular grid moves connecting the two allowable singular grids which have been altered by a singular Legendrian Riedemeister move.

Theorem 5.1. *If two allowable singular grid diagrams on the torus represent isotopic singular Legendrian links, then the two grid diagrams can be related by a sequence of Legendrian grid moves (C and S:XNW, S:XSE) and the singular grid moves (C1*, C2*, CS:X*NW, CS:X*SE, RS:X*NW, RS:X*SE).*

Proof. If Λ_1^* and Λ_2^* are two singular Legendrian links which are Legendrian isotopic, then by Theorem 4.2 they are related by a sequence of planar isotopies, Legendrian Reidemeister moves, and singular Legendrian Reidemeister moves. Theorem 3.4 gives local grid models for planar isotopies and Legendrian grid moves away from singularities. Planar isotopies near singularities can be reduced to the nonsingular case by stabilizing near the singularity. It thus suffices to provide singular grid diagram representatives of the singular Legendrian Reidemeister moves.

For $SLRM1$, we show only the case where the orientation near the singularity matches the grid configuration where the O markings are on opposite sides of the X^* marking. To see that this is a valid restriction, notice that in Figure 19, each of the local models for the orientation near X^* corresponds to this restriction, as can be seen in Figure 31. If a there is a different allowable configuration near the singularity, we can put the allowable grid diagram in this position by applying a sufficient number of cyclic permutations.

For convenience, label the O markings connected to the singular X^* as O_1, O_2, O_3, O_4, starting on the topmost O marking and labeling counterclockwise. Let X_{21} be the X marking in the same column as O_2 and let O_{21} be the O marking in the same row as X_{21}. Let X_5 and O_5 be the markings in the straight segment that is to be commuted past the singularity. By stabilizing, and up to orientation on the segment between X_5 and O_5, assume that the diagram starts by looking like the first diagram in Figure 31. The

following grid moves models a SLRM1 move (for visualization, see Figure 31),

1. Apply a $RS : X^*NW$ move.
2. Commute the row connecting X_5 and O_5 upwards by applying a C1* move.
3. Destabilize with a $RS : X^*SE$ move.

For $SLRM2$, we also show only the case where the orientation near the singularity matches the grid configuration where the O markings are on opposite sides of the X^* marking, for the same reason as before. For convenience, label the O markings connected to the singular X^* as O_1, O_2, O_3, O_4, starting on the topmost O marking and labeling counterclockwise. For the O_1 marking, keep track of the corresponding X marking in the same row (labeled X_{11}), and for the O_2 marking, keep track of the corresponding X marking in the same column (labeled X_{21}). The following grid moves models a $SLRM2$ move (for a visualization, see Figure 32),

1. Apply $CS : X^*NW$ and $RS : X^*NW$.
2. At X_{11} and X_{21} perform $S : XNW$ stabilizations.
3. For the column in the X_{11} stabilization which contains the adjacent X and O markings, commute and cyclically permute to the right until the column is adjacent to the column containing O_1. Similarly, with the row in the X_{21} stabilization that contains the adjacent X and O markings, commute and cyclically permute down until the row is adjacent to the row containing O_2. Notice here that if the X_{11} and X_{21} configuration is opposite that of Figure 32, then cyclic permutation will not be necessary.
4. In the row containing O_1, apply C2* as necessary until O_1 and O_3 are adjacent. Similarly, in the column containing O_2, apply C2* as necessary until O_2 and O_4 are adjacent. □

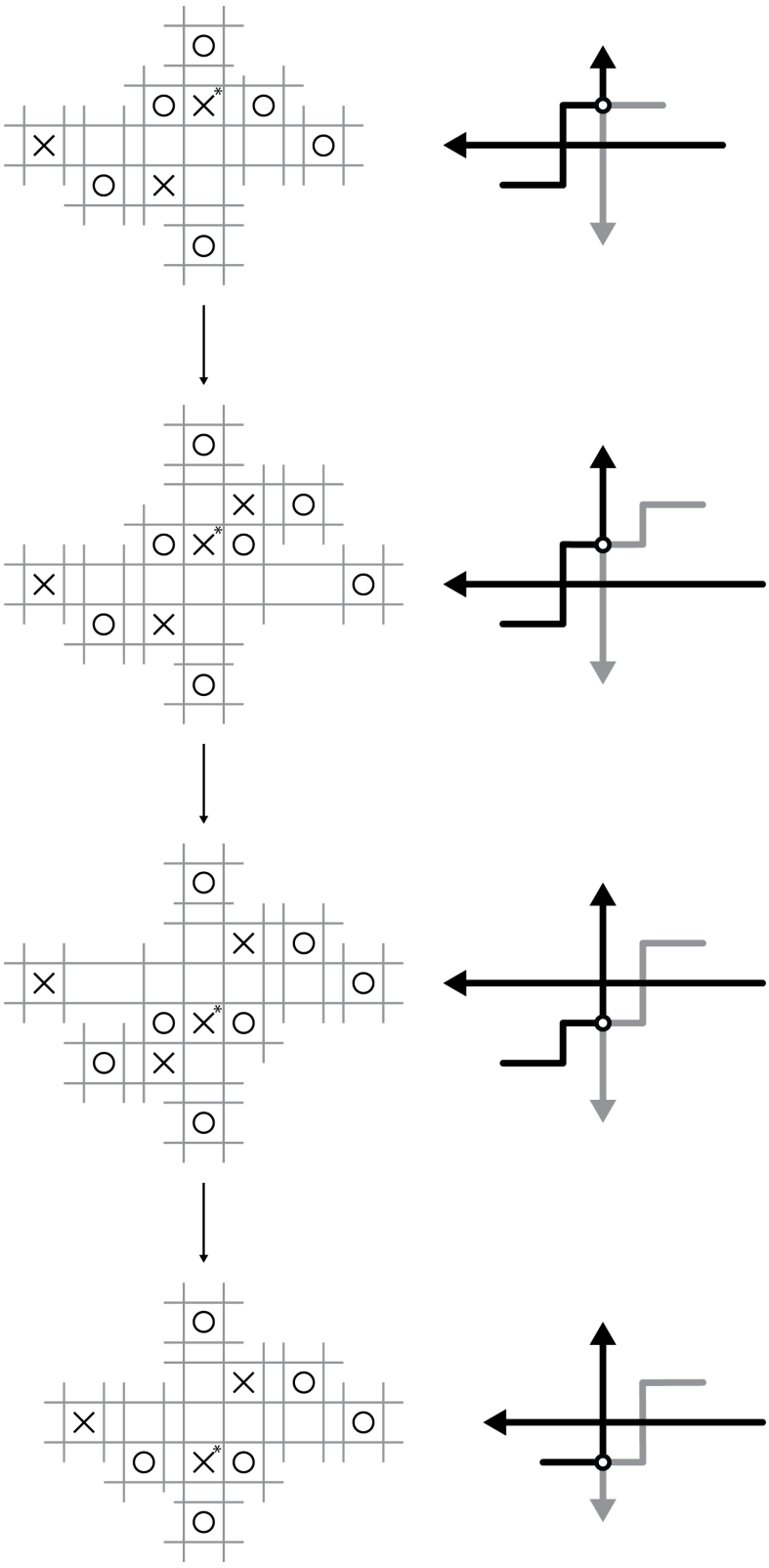

Figure 31: Grid Representation of $SLRM1$

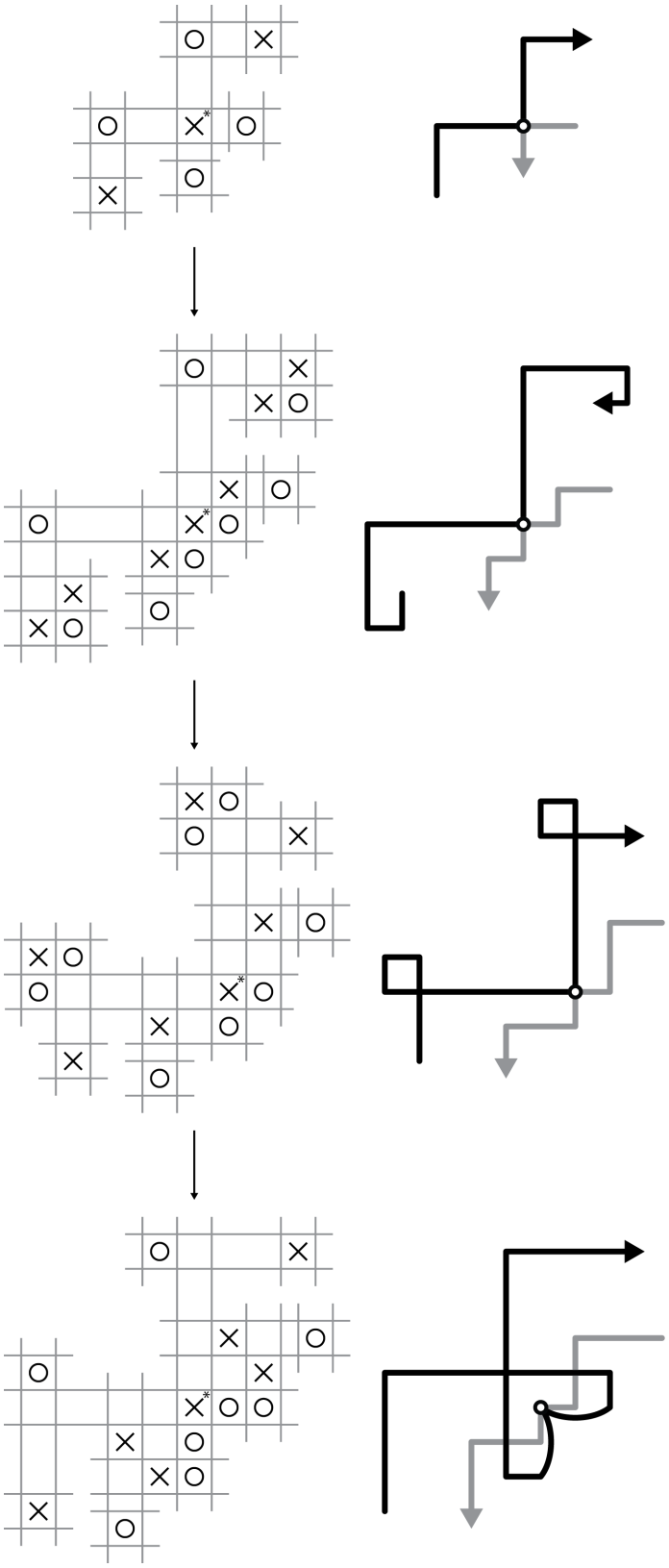

Figure 32: Grid Representation of $SLRM2$

6 Graph Grid Homology and Singular Grid Invariants

Now that all of the moves necessary four our setting are described, and we have determined how allowable singular grid diagrams of isotopic singular Legendrian links are related, we proceed to discussing singular grid homology and the singular grid invariants.

First, we present the graph grid construction given by Harvey-O'Donnol in [8] and discuss how it compares to our allowable singular grid diagrams using a natural generalization of grid homology for links. In their construction, they produce a homology invariant for transverse spatial graphs. Transverse spatial graphs differ from singular links in that there is an additional Reidemeister move near singularities. This additional move exists for graphs because the strand information, i.e. which entering strand corresponds with which exiting strand, near the singularity does not affect the graph type, while it does affect the singular link type.

We then will recount their graph grid homology definition, and apply it directly to our setting to get a grid homology theory for allowable singular grid diagrams. Last, we will define the singular Legendrian invariant from the graph grid homology, which is defined in a similar manner to the non-singular Legendrian grid invariants of Ozsváth, Szabó, and Thurston defined in [24].

Notice that in [8], the role of the X and O markings are opposite our construction. This change is to allow for a straightforward definition of the singular grid invariant. When recalling any definition or construction due to [8], we will swap the roles of the X and O markings to make the definitions more parallel to the definitions we have used.

6.1 Graph Grid Diagrams and Graph Moves

A *graph grid diagram* is an $(n \times n)$ grid in the plane, along with a set of n X markings and a set of m O markings, where $m \geq n$, so that the following rules hold,

- Each row and column contains exactly one X marking.

- Each row and column may have one or more O markings. Any X marking in the same row or column as more than one O marking will be decorated with an $*$.
- A square in the grid contains at most one marking.

Comparing this definition with the singular grid diagram definition, notice that an X^* marking can have a different number of O markings in its corresponding row and column, it need not have exactly two. Just as with the case of a singular grid diagram, a graph grid diagram uniquely describes a graph, using the same conventions as the singular grid diagram uses to describe a singular link.

Notice here that any graph described by a graph grid diagram must be sourceless and sinkless, as there must always be at least one incoming and at least one outgoing strand associated to each singularity.

In [8], they describe graph grid moves, which correspond to graph Reidemeister moves. In the graph setting, the collection of moves is more general than what is needed for allowable singular grid diagrams, and in fact, some of the moves for graphs do not give grid diagrams which represent isotopic singular links.

In addition to the non-singular grid moves, the first graph move described in [8] is the commutation$'$ move. In fact, the commutation$'$ move describes the $C1^*$, $C2^*$, and $C3^*$ moves we have defined in Section 5.1. According to Theorem 5.1, only $C1^*$ and $C2^*$ are needed to obtain isotopic singular Legendrian links. In fact, $C3^*$ does not preserve the underlying link type.

Moreover, the stabilization$'$ move described in [8] is also a generalization of our singular row and column stabilizations. Figure 33 shows an example of a stabilization$'$ move that is not one of the singular row or column stabilizations. In fact, performing such a stabilization$'$ move affects the singular link type, but not the underlying graph.

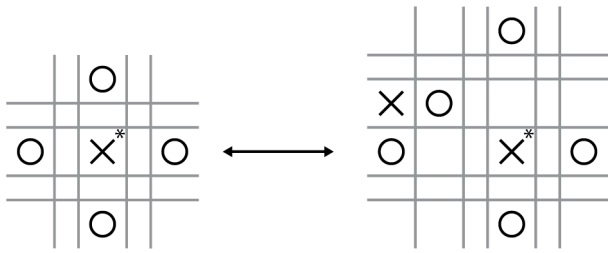

Figure 33: A Stabilization′ Move Which is Not a Singular Grid Move

6.2 Graph Grid Homology

The homology theory we will utilize in our configuration is a reworking of the graph grid homology described in [8], adapted to singular Legendrian links instead of graphs. We recall the definition here.

Let $\mathcal{G}^*$ be a graph grid diagram of size n and let $\mathbb{O} = \{O_i\}_{i=1}^m$ be an ordering on the O markings of $\mathcal{G}^*$. Just as the unblocked grid homology, the *graph grid homology* for $\mathcal{G}^*$, $SGH^-(\mathcal{G}^*)$, is defined to be the homology of the chain complex (SGC^-, ∂^-), where SGC^- is the free $\mathbb{Z}_2[V_1, ..., V_m]$-module generated by $\mathbf{S}(\mathcal{G}^*)$ and where ∂^- is defined on $\mathbf{S}(\mathcal{G}^*)$ by

$$\partial^-(\mathbf{x}) = \sum_{\mathbf{y}\in\mathbf{S}(\mathcal{G}^*)} \sum_{\{r\in \mathrm{Rect}^\circ(\mathbf{x},\mathbf{y}) \,|\, r\cap\mathbb{X}=\emptyset\}} V_1^{\mathcal{O}_1(r)} \cdots V_m^{\mathcal{O}_m(r)} \cdot y,$$

and then extended linearly to all of $\mathbb{Z}_2[V_1, ..., V_m]$.

The fact that this actually forms a chain complex and is invariant under these grid moves is largely due to Harvey-O'Donnol in [8].

Using the graph grid homology theory, one can define the singular collapsed chain complex or the singular uncollapsed chain complex for singular links in an analogous way to the non-singular setting. In fact, if $\mathcal{G}^*$ represents a knot, we can also define the singular fully blocked grid homology or the singular simply blocked grid homology.

The Harvey-O'Donnol construction of the more general graph grid homology requires that singularities be sourceless and sinkless, which is satisfied in our situation, as we are looking specifically at singular link diagrams that must have two incoming and outgoing strands.

The proof of invaraiance of the graph grid homology under Harvey-O'Donnol's commutation$'$ and stabilization$'$ moves is almost a direct translation of the proof given in [12]. The proof given in [8] provides a proof of invariance of graph grid homology under our necessary moves ($C1^*$, $C2^*$, $CS : X^*NW$, $CS : X^*SE$, $RS : X^*NW$, $RS : X^*SE$), as they each are specific cases of the commutation$'$ and stabilization$'$ moves and exchanging the role of the O^* and X^* markings does not affect the proof they provide.

6.3 Singular Legendrian Grid Invariants

Let $\mathcal{G}^*$ be an allowable singular grid diagram, and $\mathbf{x}^+$ be the grid state whose components are the NE corners of squares in $\mathcal{G}^*$ that contain either an X marking or an X^* marking, and $\mathbf{x}^-$ be the grid state whose components are in the SW corners of squares in $\mathcal{G}^*$ that contain either an X marking or an X^* marking. The homology classes of these grid states in $SGH^-(\mathcal{G}^*)$ will be denoted $\lambda^{\pm}$, and, if $\mathcal{G}^*$ represents a knot, in $\widehat{SGH}(\mathcal{G}^*)$, will be denoted $\widehat{\lambda}^{\pm}$.

Theorem 6.1. *Let $\mathcal{G}_1^*$ and $\mathcal{G}_2^*$ be two allowable singular grid diagrams that differ by a singular commutation move of type $C1^*$ or $C2^*$. Then the quasi-isomorphism $P^* : SGC^-(\mathcal{G}_1^*) \to SGC^-(\mathcal{G}_2^*)$ defined by*

$$P^*(\mathbf{x}) = \sum_{\mathbf{y}' \in \mathbf{S}(\mathcal{G}_1^*)} \sum_{\{p \in Pent^\circ(\mathbf{x},\mathbf{y}) \,|\, p \cap \mathbb{X} = \emptyset\}} V_1^{\mathcal{O}_1(p)} \cdots V_m^{\mathcal{O}_m(p)} \cdot \mathbf{y}'$$

is natural with respect to $\mathbf{x}^{\pm}$. That is, $P^*(\mathbf{x}^+(\mathcal{G}_1^*)) = \mathbf{x}^+(\mathcal{G}_2^*)$ and $P^*(\mathbf{x}^-(\mathcal{G}_1^*)) = \mathbf{x}^-(\mathcal{G}_2^*)$.

Proof. Let $\mathcal{G}_1^*$ and $\mathcal{G}_2^*$ be two singular grid diagrams which differ by a $C1^*$ move. The proof that P^* is a quasi-isomorphism is the same as the proof that P is a quasi-isomorphism in the nonsingular case, as explained in [8]. It remains to show that P^* is natural with respect to $\mathbf{x}^{\pm}$. To see this, we first set up a commutation diagram in a way analogous to that described in Figure 10. The only difference is that one of the X markings in Figure 10 has

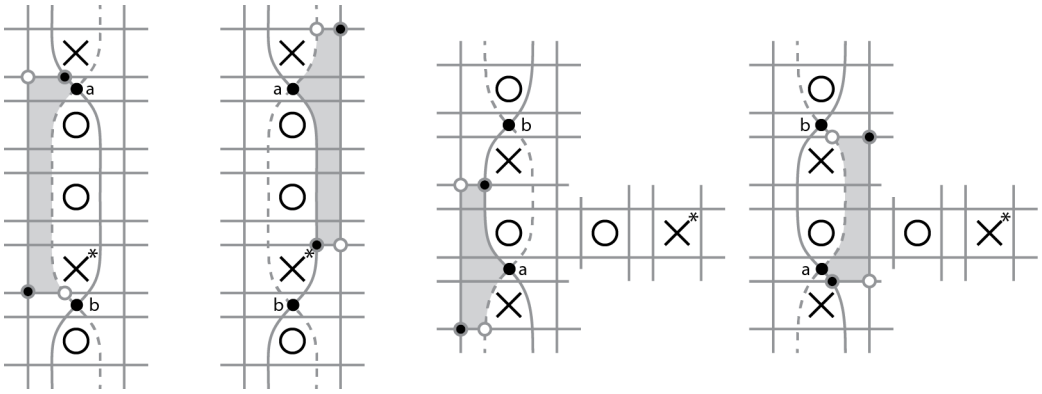

Figure 34: Pentagons Showing $P^*(\mathbf{x}^{\pm}(\mathcal{G}^*)) = \mathbf{x}^{\pm}(\mathcal{G}^{*\prime})$ for $C1^*$ and $C2^*$

become an X^* marking, according to its location in $\mathcal{G}_1^*$ and $\mathcal{G}_2^*$.

As P^* counts pentagons in the grid, let $p \in \mathrm{Pent}^{\circ}(\mathbf{x}^-, \mathbf{y}')$ be a pentagon from $\mathbf{x}^-$ to any $\mathbf{y}'$. Notice that if $\mathbf{y}'$ is any other marking than $\mathbf{x}^-(\mathcal{G}_2^*)$, then p will contain an X marking in its lower left corner, because any other pentagon leaving the marking in the SW corner of the X^* marking will contain X^*, as can be seen in Figure 34. As P^* only counts pentagons that do not intersect any X markings, the only possible $p \in \mathrm{Pent}^{\circ}(\mathbf{x}^-, \mathbf{y}')$ is the one shown on the left in Figure 34. Notice that the shaded region pictured is a pentagon according to the definition given in Section 2.5. The argument for $\mathbf{x}^+$ and C2* is similar, and their respective pentagons can be seen in Figure 34.

□

Theorem 6.2. *Let $\mathcal{G}_1^*$ be a singular grid diagram and $\mathcal{G}_2^*$ be obtained from $\mathcal{G}_1^*$ by a stabilization of type $CS : X^*NW$, $CS : X^*SE$, $RS : X^*NW$ or $RS : X^*SE$. Then there is an isomorphism $\Phi : SGH^-(\mathcal{G}_1^*) \to SGH^-(\mathcal{G}_2^*)$ so that $\Phi(\lambda^+(\mathcal{G}_1^*)) = \lambda^+(\mathcal{G}_2^*)$ and $\Phi(\lambda^-(\mathcal{G}_1^*)) = \lambda^-(\mathcal{G}_2^*)$.*

Proof. Let $\mathcal{G}_1^*$ and $\mathcal{G}_2^*$ be two singular grid diagrams which differ by a stabilization of one of the listed types. Adapting Proposition 2.8, as is done in [8], gives an isomorphism of $SGH^-(\mathcal{G}_2^*) \cong SGH^-(\mathcal{G}_1^*)$. It suffices to show that the image of $\mathbf{x}^{\pm}(\mathcal{G}_2^*)$ under the map e is $\mathbf{x}^{\pm}(\mathcal{G}_1^*)$, where e is as used in Proposition 2.8. Since e is an isomorphism of chain

complexes, $e : \mathbf{I} \to SGC^-(\mathcal{G}_1^*)[V_1]$ induced by the one-to-one correspondence between $\mathbf{I}(\mathcal{G}_2^*)$ and $\mathbf{S}(\mathcal{G}_1^*)$, the grid states $\mathbf{x}^{\pm}(\mathcal{G}_1^*)$ are mapped to $\mathbf{x}^{\pm}(\mathcal{G}_2^*)$ under the inverse e', since the addition of point c is in both the northeast and southwest corners of X marked squares. □

Theorem 6.3. *Suppose Λ_1^* and Λ_2^* are singular Legendrian links that are Legendrian isotopic with allowable singular grid representatives $\mathcal{G}_1^*$ and $\mathcal{G}_2^*$, respectively. Then there is an isomorphism $\phi : SGH^-(\mathcal{G}_1^*) \to SGH^-(\mathcal{G}_2^*)$ where $\phi(\lambda^+(\mathcal{G}_1^*)) = \lambda^+(\mathcal{G}_2^*)$ and $\phi(\lambda^-(\mathcal{G}_1^*)) = \lambda^-(\mathcal{G}_2^*)$.*

Proof. Theorem 5.1 shows that $\mathcal{G}_1^*$ and $\mathcal{G}_2^*$ must be related by a sequence of C, $S : XNW$, $S : XSE$, $C1^*$, $C2^*$, $CS : X^*NW$, $CS : X^*SE$, $RS : X^*NW$, or $RS : X^*SE$ moves. Thus, it suffices to show that each of these moves individually give isomophisms that are natural with respect to $\lambda^{\pm}$.

C, $S : XNW$, and $S : XSE$ were shown to induce an isomorphsim in Theorem 3.5. The pentagon map was used to show that $C1^*$ and $C2^*$ are natural with respect to $\mathbf{x}^{\pm}$, and it induces a quasi-isomorphism, in Theorem 6.1. For the stabilizations of types $CS : X^*NW$, $CS : X^*SE$, $RS : X^*NW$, and $RS : X^*SE$, it was shown in Theorem 6.2 that these induce such an isomorphism. Since $\mathcal{G}_1^*$ and $\mathcal{G}_2^*$ are related by a finite sequence of these moves, each of which induce an isomorphism on homology, composing these isomorphisms results in the desired Φ. □

Corollary 6.4. *Suppose Λ_1^* and Λ_2^* are singular Legendrian links that are Legendrian isotopic with singular grid representatives $\mathcal{G}_1^*$ and $\mathcal{G}_2^*$, respectively. Then there is an isomorphism $\phi : \widehat{SGH}(\mathcal{G}_1^*) \to \widehat{SGH}(\mathcal{G}_2^*)$ where $\phi(\widehat{\lambda}^+(\mathcal{G}_1^*)) = \widehat{\lambda}^+(\mathcal{G}_2^*)$ and $\phi(\widehat{\lambda}^-(\mathcal{G}_1^*)) = \widehat{\lambda}^-(\mathcal{G}_2^*)$, where $\widehat{\lambda}^{\pm}$ is the homology class in $\widehat{SGH}$ represented by $\mathbf{x}^{\pm}$.*

Proof. The sequence of isomorphisms from Theorem 5.5 are induced by a sequence of quasi-isomorphisms of the chain complex SGC^-. Adapting these quasi-isomophisms to $\widehat{SGC}$ in the case where $\mathcal{G}_1^*$ and $\mathcal{G}_2^*$ represent knots, then gives an isomorphism as desired. □

Bibliography

[1] B. An, Y. Bae, and S. Kim. Legendrian singular links and singular connected sums. *Journal of Symplectic Geometry*, 16(4):885–930, 2018.

[2] B. An and H. Lee. Grid diagram for singular links. *Journal of Knot Theory and Its Ramifications*, 27(04):1850023, Apr 2018.

[3] B. Audoux. Singular link Floer homology. *Algebraic & Geometric Topology*, 9(1):495–535, Mar 2009.

[4] S. Baader and M. Ishikawa. Legendrian graphs and quasipositive diagrams. *Annales de la faculté des sciences de Toulouse Mathématiques*, 18(2):285–305, 2009.

[5] Y. Chekanov. Differential algebras of legendrian links. *Inventiones Mathematicae*, 150(3):441–482, Dec 2002.

[6] P. Cromwell. Embedding knots and links in an open book i: Basic properties. *Topology and its Applications*, 64(1):37–58, 1995.

[7] John B. Etnyre. Legendrian and transversal knots. *Handbook of Knot Theory*, page 105–185, 2005.

[8] S. Harvey and D. O'Donnol. Heegaard floer homology of spatial graphs. *Algebraic & Geometric Topology*, 17(3):1445–1525, Jul 2017.

[9] L. Kauffman. Invariants of graphs in three-space. *Transactions of The American Mathematical Society*, 311(2):697–710, Feb 1989.

[10] P. Lisca, P. Ozsváth, A. Stipsicz, and Z. Szabó. Heegard Floer invariants of Legendrian knots in contact three-manifolds. *Journal of the European Mathematical Society*, 11(6):1307–1363, 2009.

[11] C. Manolescu, P. Ozsváth, and S. Sarkar. A combinatorial description of knot Floer homology. *Annals of Mathematics*, 169(2):633–660, Mar 2009.

[12] C. Manolescu, P. Ozsváth, Z. Szabó, and D. Thurston. On combinatorial link Floer homology. *Geometry & Topology*, 11(4):2339–2412, Dec 2007.

[13] D. McDuff and A. D. Salamon. *Introduction to Symplectic Topology*, volume 27 of *Oxford Graduate Texts in Mathematics*. Oxford University Press, 2017.

[14] J. Moser. On the volume elements on a manifold. *Transactions of the American Mathematical Society*, 120(2):286–294, 1965.

[15] L. Ng and D. Thurston. Grid diagrams, braids, and contact geometry. *Proceedings of Gökova Geometry-Topology Conference 2008*, pages 120–136, 2008.

[16] Y. Ni. Knot Floer homology detects fibred knots. *Inventiones mathematicae*, 170(3):577–608, Sep 2007.

[17] B. Owens. Unknotting information from Heegaard Floer homology. *Advances in Mathematics*, 217(5):2353–2376, Mar 2008.

[18] P. Ozsváth, A. Stipsicz, and Z. Szabó. Floer homology and singular knots. *Journal of Topology*, 2(2):380–404, 2009.

[19] P. Ozsváth, A. Stipsicz, and Z. Szabó. *Grid Homology for Knots and Links*, volume 208 of *Mathematical Surveys and Monographs*. American Mathematical Society, 2015.

[20] P. Ozsváth and Z. Szabó. Holomorphic disks and knot invariants. *Advances in Mathematics*, 186(1):58–116, Aug 2004.

[21] P. Ozsváth and Z. Szabó. Holomorphic disks and three-manifolds invariants: properties and applications. *Annals of Mathematics*, 159(3):1159–1245, May 2004.

[22] P. Ozsváth and Z. Szabó. Holomorphic disks and topological invariants for closed three-manifolds. *Annals of Mathematics*, 159(3):1027–1158, May 2004.

[23] P. Ozsváth and Z. Szabó. Holomorphic disks, link invariants and the multi-variable Alexander polynomial. *Algebraic & Geometric Topology*, 8(2):615–692, May 2008.

[24] P. Ozsváth, Z. Szabó, and D. Thurston. Legendrian knots, transverse knots and combinatorial Floer homology. *Geometry & Topology*, 12(2):941–980, May 2008.

[25] J. Rasmussen. *Floer homology and knot complements*. PhD thesis, Harvard University, May 2003.

[26] K. Reidemeister. *Knotentheorie*, volume 1 of *Ergebnisse der Mathematik und ihrer Grenzgebiete. 2. Folge*. Springer-Verlag Berlin Heidelberg, 1932.

[27] S. Sarkar and J. Wang. An algorithm for computing some Heegaard Floer homologies. *Annals of Mathematics*, 171(2):1213–1236, Mar 2010.

[28] J. Swiatkowski. On the isotopy of Legendrian knots. *Annals of Global Analysis and Geometry*, 10(3):195–207, Jan 1992.

[29] S. Welji. *On the Heegaard Floer homology of singular knots and their unoriented resolutions*. PhD thesis, Columbia University, 2009.